Achievements, Challenges, and Prospects of Calcium Batteries

Downloaded from: https://research.chalmers.se, 2026-04-05 08:34 UTC

Citation for the original published paper (version of record):

Arroyo-De Dompablo, M., Ponrouch, A., Johansson, P. et al (2020). Achievements, Challenges, and Prospects of Calcium Batteries. Chemical Reviews, 120(14): 6331-6357. http://dx.doi.org/10.1021/acs.chemrev.9b00339

N.B. When citing this work, cite the original published paper.

research.chalmers.se offers the possibility of retrieving research publications produced at Chalmers University of Technology. It covers all kind of research output: articles, dissertations, conference papers, reports etc. since 2004. research.chalmers.se is administrated and maintained by Chalmers Library

(article starts on next page)

This is an open access article published under an ACS AuthorChoice License, which permits copying and redistribution of the article or any adaptations for non-commercial purposes.

CHEMICAL REVIEWS

Review

Cite This: Chem. Rev. 2020, 120, 6331−6357

pubs.acs.org/CR

Achievements, Challenges, and Prospects of Calcium Batteries

M. Elena Arroyo-de Dompablo,*,† Alexandre Ponrouch,‡,§ Patrik Johansson,§,∥ and M. Rosa Palacín*,‡,§

†Departamento de Química Inorgánica, Universidad Complutense de Madrid, Avda. Complutense sn, 28040 Madrid, Spain

‡Institut de Ciència de Materials de Barcelona (ICMAB-CSIC) Campus UAB, 08193 Bellaterra, Catalonia, Spain

§ALISTORE-European Research Institute, CNRS FR 3104, Hub de l'Energie, 15 Rue Baudelocque, 80039 Amiens, France

∥Department of Physics, Chalmers University of Technology, 41296 Gothenburg, Sweden

ABSTRACT: This Review flows from past attempts to develop a (rechargeable) battery technology based on Ca via crucial breakthroughs to arrive at a comprehensive discussion of the current challenges at hand. The realization of a rechargeable Ca battery technology primarily requires identification and development of suitable electrodes and electrolytes, which is why we here cover the progress starting from the fundamental electrode/electrolyte requirements, concepts, materials, and compositions employed and finally a critical analysis of the state-of-the-art, allowing us to conclude with the particular roadblocks still existing. As for crucial breakthroughs, reversible plating and stripping of calcium at the metal-anode interface was achieved only recently and for very specific electrolyte formulations. Therefore, while much of the current research aims at finding suitable cathodes to achieve proof-of-concept for a full Ca battery, the spectrum of electrolytes researched is also expanded. Compatibility of cell components is essential, and to ensure this, proper characterization is needed, which requires design of a multitude of reliable experimental setups and sometimes methodology development beyond that of other next generation battery technologies. Finally, we conclude with recommendations for future strategies to make best use of the current advances in materials science combined with computational design, electrochemistry, and battery engineering, all to propel the Ca battery technology to reality and ultimately reach its full potential for energy storage.

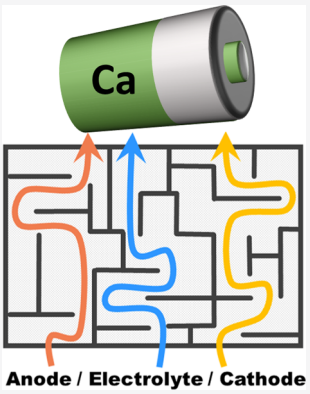

CONTENTS

1. INTRODUCTION

Efficient and readily available energy storage is essential to help solving some of the grand challenges our modern society is facing today: air pollution, oil-dependency, and climate change. The magnitude of the challenge is huge and involves many interrelated aspects including energy independence, environmental sustainability, economics—and not the least technological development. Electrochemical energy storage is considered to be a key technology, and the prevailing lithium-ion battery (LIB) technology has made possible our society of portable electronic devices. It also offers a near-term solution for more sustainable transport with less environmental impact and stationary energy storage for renewable energies, such as solar and wind power. While the cost of LIBs has been reduced by 8% at the pack level annually during the past decade,[1] this technology is now reaching its fundamental limits in terms of

Special Issue: Beyond Li-Ion Battery Chemistry

Received: May 27, 2019
Published: October 29, 2019

See https://pubs.acs.org/sharingguidelines for options on how to legitimately share published articles.

© 2019 American Chemical Society

DOI: 10.1021/acs.chemrev.9b00339
Chem. Rev. 2020, 120, 6331−6357

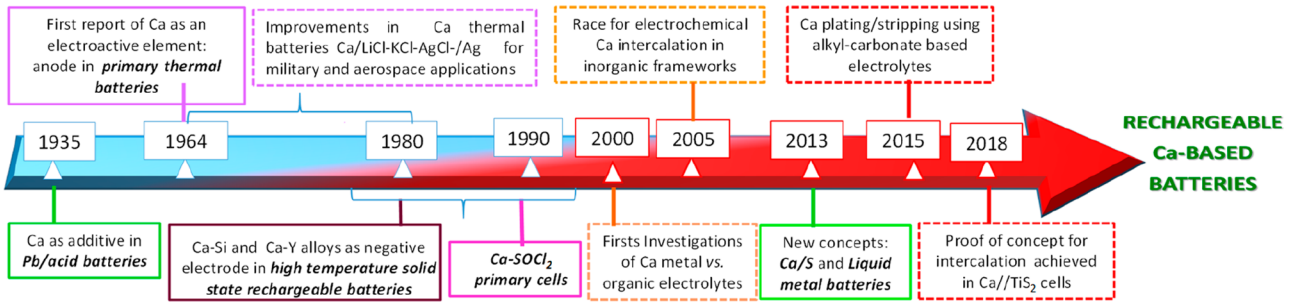

Figure 1. Timeline of Ca use in battery technologies.

energy density. In addition, while the quest for even higher energy densities has for long been the main driving force behind progress in battery technology, LIBs contain both Ni and Co, and the risks of limited supply and/or significantly increased prices cannot be ignored and prompt the development of more long-term sustainable battery chemistries.[2,3] Furthermore, a transition from metal ion- to metal-anode-based battery chemistries is appealing, as it can substantially enhance the figures of merit.[4−8] If also more abundant and nontoxic metals are used, the overall battery technology would also benefit from reduced cost and lower environmental impact. Moreover, the concept becomes particularly attractive if multivalent ions are used as charge carriers, as this in principle enables the capacities to be doubled as compared to using monovalent-ion charge carriers such as Li^+ or Na^+. Alternatively, one can consider that reaction of only a half of the ions would be needed to achieve the same capacity.[8,9] Combining all of the above: Calcium is the fifth most abundant element in the Earth's crust, it is nontoxic, and its standard reduction potential is −2.87 vs NHE, which combined with its density of 1.54 g/cm^3 and charge capacity of 1.34 Ah/g, result in a theoretical energy density of 2.06 Ah/cm^3. In comparison, the graphite of today's LIBs is at a mere 0.97 Ah/cm^3—hence a 2-fold increase in this measure is achievable. In addition, the Ca^{2+} ion should be more mobile in liquid electrolytes because of its less polarizing character (charge/radius ratio) than both Mg^{2+} and Al^{3+} ions, which are employed in battery concepts much more heavily researched. To enable the reader to more easily understand the (limited) development of Ca batteries until now, we here first provide a historical perspective before we turn to the (rapid) progress during the last 4 years.

This Review presents a comprehensive examination of the requirements and current state-of-the-art of electrolytes and electrodes for rechargeable Ca batteries. This section contains a minor historical recollection, section 2 covers the exploration of active materials and electrolytes, while section 3 deals with the (un)reliability of experimental setups used and the methodology development needed, before we assess full-cell layouts and finally present some concluding remarks.

1.1. Historical Perspective (−2015): A Myriad of Concepts

The first application of calcium at all in batteries was in 1935 but then as an additive for alloy strengthening the lead grids for Pb−acid battery cells.[10−12] The first report of calcium as the electroactive element appeared much later, in 1964, and is related to primary thermal batteries, a technology mostly used in military and aerospace applications (Figure 1).[13] These Ca batteries contained electrolytes with high melting points (such as mixtures of metal chlorides), kept at ambient temperature during storage periods (which may be extremely long) to avoid self-discharge and thermally activated to deliver power. The Ca/KCl−LiCl−AgCl−K_2CrO_4/Ag cells were reported to discharge at 450 °C for 11 min, despite issues related to the formation of a Li−Ca alloy at the anode. This type of cell was used in military applications since World War II.[14] Some attempts to modify the surface of the calcium metal anodes with acetic acid to yield $CaCO_3$ were reported,[15] despite the chemistry being shown to be extremely complex involving also corrosion with formation of both Ca_2CrO_4Cl and $KCaCl_3$.[16] Efforts to replace the chlorides by nitrates, with lower melting points, as electrolytes were also reported.[17] A maximum exchange of one electron per mole of calcium was observed with the formation of a passivation film most likely consisting of CaO, hindering any fast kinetics. The addition of halides to the electrolyte was suggested as a way to break the passivation film and improve the kinetics. Other high-temperature concepts investigated in these early days involved the use of a Ca−Si alloy anode coupled to a Ca^{2+} conducting β''-alumina solid electrolyte for rechargeable cells operating at 580 °C,[18] a Ca−Y alloy anode coupled to a fluoride conducting solid electrolyte,[19] and even a Ca−O_2 cell−also using a Ca−Si alloy anode complement with a zirconia-based electrolyte.[20] Despite a few charge−discharge cycles being reported for the above systems, the redox mechanism was not unambiguously ascertained, and no further studies were published.

Staniewicz was the first to report on the electrochemistry of Ca−$SOCl_2$ as an alternative to the Li−$SOCl_2$ primary cells, again a battery technology mainly used for military applications, and presented the impossibility of calcium plating upon cell reversal as a safety advantage.[21] Further studies by Peled et al. attributed this feature to the formation of a passivation layer consisting mainly of $CaCl_2$ impermeable to the Ca^{2+} ions.[22−25] A similar technology with a somewhat higher operation cell potential was also developed,[26,27] but corrosion of the Ca metal electrodes was found to be an issue; the Ca−$SOCl_2$ cells lost ca. 10% of their capacity after only 2 weeks of storage.[28] The strategy to avoid corrosion and self-discharge was to use different additives such as $Ca(AlCl_4)_2$ formed by reacting Ca with $AlCl_3$,[21] $Sr(AlCl_4)_2$, or $Ba(AlCl_4)_2$, changing the composition of the passivation layer.[29] Furthermore, corrosion of the stainless steel can material was also observed and attributed to reactivity with calcium metal, in analogy with lithium metal systems.[30] As the calcium-based concepts above did not provide enough advantages to replace the Li−$SOCl_2$ technology, they never reached the market,[31] but this may also be related to the fact that these batteries are only used in niche applications (military or very low-temperature environments).

The issues related to electrochemical calcium deposition discovered in the studies above effectively prevented any further investigations of secondary, rechargeable, battery technologies based on calcium metal as the negative electrode. Yet, basic

DOI: 10.1021/acs.chemrev.9b00339
Chem. Rev. 2020, 120, 6331−6357

studies related to the behavior of calcium metal anodes using organic electrolytes similar to those used at the time of emerging LIB technology were made by Aurbach et al.[32] Their studies included solvents such as acetonitrile (ACN), tetrahydrofuran (THF), γ-butyrolactone (gBL), and propylene carbonate (PC) as well as $Ca(ClO_4)_2$ and $Ca(BF_4)_2$ salts together with noncalcium containing salts. The conclusion of this pioneering work was that the passivation layer formed on calcium metal does not enable transport of calcium ions, in full agreement with the results for the $SOCl_2$ battery technology, with the major consequence being the impossibility to develop any secondary Ca batteries using these electrolytes, as even if calcium stripping would be feasible, plating upon charge would not. By the year 2000, when the LIB technology was already well-established in the market,[33] the idea to use metal anodes coupled to multivalent-ion charge carriers re-emerged as a way to further boost the energy density. Indeed, proof-of-concept was achieved for Mg battery cells with metal anodes,[34] using magnesium organohaloaluminate salts in THF or glymes as electrolytes, which, despite a somewhat narrow electrochemical stability window of ca. 3 V, enabled reversible Mg plating and stripping. Yet, no similar electrolytes were available for Ca,[8] and hence, the study of Ca^{2+} intercalation and the quest for cathodes was not straightforward, the only possibility being the assembly of cells using alternative anodes, such as activated carbon.[35]

The basics of calcium-ion intercalation in transition-metal compounds were studied in the 1960s−1970s as part of early intercalation chemistry research.[36] This involved crystal structures exhibiting a van der Waals gap, such as metal sulfides WS_2, TaS_2, TiS_2, and some metal oxides, e.g., MoO_3, and V_2O_5, in which intercalation of a wide range of neutral or charged species was possible, the latter concomitant to reduction of the transition metal of the host. Despite most studies being devoted to intercalation of lithium and other alkali ions, attempts to chemically intercalate other ions such as Ca^{2+} for comparative purposes were common, either from aqueous solutions of the corresponding hydroxides or from the metal dissolved in liquid ammonia.[37−39] Due to the advent of the LIB technology in the 1970s, which concentrated most research efforts to Li^+, research on multivalent systems fell into oblivion, but the field started to re-emerge in the early 2000s, with a few reports dealing with the feasibility of calcium intercalation in inorganic compounds. These included electrochemical studies of hexacyanoferrates using an aqueous electrolyte[40,41] and combining electrochemistry and other characterization techniques (mostly powder X-ray diffraction, or XRD hereafter) with V_2O_5 as the host using $Ca(ClO_4)_2$ in either ACN or PC as electrolytes.[42−44]

In the following decade and in line with the growing awareness about the imperative evolution toward electrification of transportation and energy storage needs for renewable energy, the efforts in the area were reinforced. This resulted in investigations of new concepts such as Ca/S cells,[45] which showed some electrochemical response but lacked reversibility, and more exotic alternatives such as liquid metal batteries.[46] The latter concept consists of two liquid metal electrodes separated by a molten salt electrolyte that self-segregate into three liquid layers based on immiscibility and density differences. While the solubility in molten salts and strong reducing power of Ca preclude its use as metal electrode, calcium containing alloys melting at moderate temperatures (around 600 °C) seem to exhibit promising behavior using molten halide electrolytes[47−49] given their thermodynamic redox potential,[50,51] but much engineering is needed for this technology—development of corrosion resistant cell components, effective seals, and thermal management, and so on—before any proper practical estimates can be made.

Reinvestigations of hexacyanoferrates were also made using both aqueous[41] and organic[52] electrolytes resulting in a very reversible electrochemical response and with enhanced capacity obtained by water addition to the organic electrolytes.[53] Despite some further studies,[54,55] indicating minor, if any, modifications of the host structural framework, the redox mechanism and the possible role of water molecules, either present in the as prepared hexacyanoferrates or in the electrolyte, have not yet been fully elucidated. Interest in intercalation cathodes, such as those used in the LIB technology and using the vast know-how created in that field, also re-emerged, but the bottlenecks related to the differences between Li^+ and Ca^{2+} as charge carriers were soon clearly realized and hence the need for specific materials design.[56,57]

1.2. The Current Era (2016−): Realizing Metal-Anode- and Organic-Electrolyte-Based Cells

By the end of 2015, the feasibility of reversible calcium metal plating and stripping was assessed at moderate temperatures using conventional alkyl-carbonate organic-solvent-based electrolytes.[58] Despite issues associated with these electrolytes, this opened for a more extensive electrode materials screening. With Ca metal anodes being the most attractive choice, research was focused on electrolyte formulations enabling better Coulombic efficiency and, if possible, making operation at room temperature feasible, and at the same time, these were used for unraveling suitable cathode materials. Yet, alternative anodes have also been researched; the first calcium graphite intercalation compound (CaC_6) was achieved chemically at high temperature in 2005[59] and attempted electrochemically somewhat later.[60] An interest in Ca alloys has been present since 2011,[61] but still, most efforts are directed toward cells using calcium metal anodes and intercalation cathodes.[62]

Most Ca battery cells are analogous with LIBs on the cathode side; during the discharge, the charge carrier ion (Ca^{2+}) migrates from the anode to the cathode through the electrolyte, while the electrons flow across an external circuit (Figure 2). These

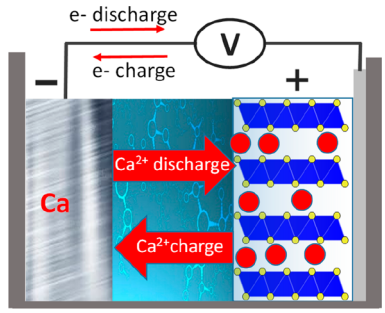

Figure 2. Schematic of a Ca battery using a Ca metal anode and an intercalation cathode.

processes are reversed upon charging. Except for a few more exotic concepts, with air[63,64] or sulfur cathodes,[45] the redox mechanism at the cathode involves insertion/deinsertion of Ca^{2+}

$$x\mathrm{Ca}^{2+} + 2x\mathrm{e}^- + \mathrm{Ca}_y\mathrm{Host} \Leftrightarrow \mathrm{Ca}_{x+y}\mathrm{Host} \quad (1)$$

where Host represents the cathode active material wherein the Ca^{2+} ions are intercalated. For Ca batteries, the main challenge is

DOI: 10.1021/acs.chemrev.9b00339
Chem. Rev. 2020, 120, 6331−6357

Table 1. Electrochemical Tests of Ca Anodes in Two- or Three-Electrode Cells

negative/working electrode	counter electrode	reference electrode	electrolyte	cutoff voltage (cyclic voltammetry)	passivation	coulombic efficiency	number of cycles	water content (ppm)	comments
Ca[21]	$SOCl_2$/C	Ca	$Ca(AlCl_4)_2$ in $SOCl_2$		$CaCl_2$	<5%	0	-	Ca stripping at ca. 100 mV vs Ca pseudo-RE.
Ca or Au[32]	Ca	Ca	0.05 to 1 M $Ca(ClO_4)_2$ or $Ca(BF_4)_2$ in THF, PC, γBL, or ACN	−1.8 V vs Ca pseudo-RE	$CaCl_2$ in ClO_4-based electrolyte, $Ca(OH)_2$ in THF	0%	1	<30	No plating observed. Shift of the Ca metal RE: 750 mV.
Ca[74]	Ca	Ca	0.45 M $Ca(BF_4)_2$ in EC:PC (100 °C)	−1.4 V vs Ca metal	borate, carbonate, CaF_2	85%	30	<40	Plating observed above 75 °C.
Au[73]	Ca	Ca	1.5 M $Ca(BH_4)_2$ in THF		CaH_2	95%	50	<4	
Pt[79]	Ca	Ca	0.25 M CaBhfip in DME	−0.35 V vs Ca metal	CaF_2	80%	22	-	5 CV cycles at 80 $mV{\cdot}s^{-1}$ conditioning procedure.
Au[78]	Ca	Ca	0.5 M CaBhfip + 0.1 M Bu_4NCl in DME	−1.0 V vs Ca metal	CaF_2	90%	50	-	Bu_4NCl appeared mandatory for long-term cycling.
$CaSi_2$[58]	Ca	Ca	0.45 M $Ca(BF_4)_2$ in EC:PC (100 °C)	0.8 V vs Ca metal			1	<30	Dealloying evidenced by XRD, alloy formation at very high overpotential.
Sn[81,82] fully reduced: Ca_7Sn_6 (?)	graphite and activated carbon	-	0.8 M $Ca(PF_6)_2$ in EC:PC:DMC:EMC (2:2:3:3 in vol)	5 V for full cells	carbonate and CaF_2	ca. 80%	350 and 1000	-	Stability issues of $Ca(PF_6)_2$ and cell balancing? Long cycling only at high C-rate (low Coulombic efficiency at low C-rate).
GeO_2[98]	graphite rod	pyres-glass sealed Ag/AgCl	$CaCl_2$−NaCl (1:1) melt at 600 °C	−2.5 V vs Ag/AgCl			1		Absence of Na alloy was ascertained by means of EDX and XRD.
MCMB[89]	expanded graphite	-	0.8 M $Ca(PF_6)_2$ in EC:DMC:EMC (5:3:2 vol)	5.2 V for full cells		ca. 80%	300	-	Stability issues of $Ca(PF_6)_2$ and cell balancing? Long cycling only at high C-rate (low Coulombic efficiency at low C-rate).
PNDIE[97]	copper hexacyanoferrate	Ag/AgCl	2.5 M $Ca(NO_3)_2$ (aq) (pH = 5.1)	−0.9 V vs Ag/AgCl		99% (at C/2)	2000	-	Role of proton studied by cycling at pH 3, 5, 7, and 9.
PTCDA[96]	activated carbon	-	$Ca(NO_3)_2$ (aq) sat.				10	-	Amorphization upon cycling. HER?

DOI: 10.1021/acs.chemrev.9b00339
Chem. Rev. 2020, 120, 6331−6357

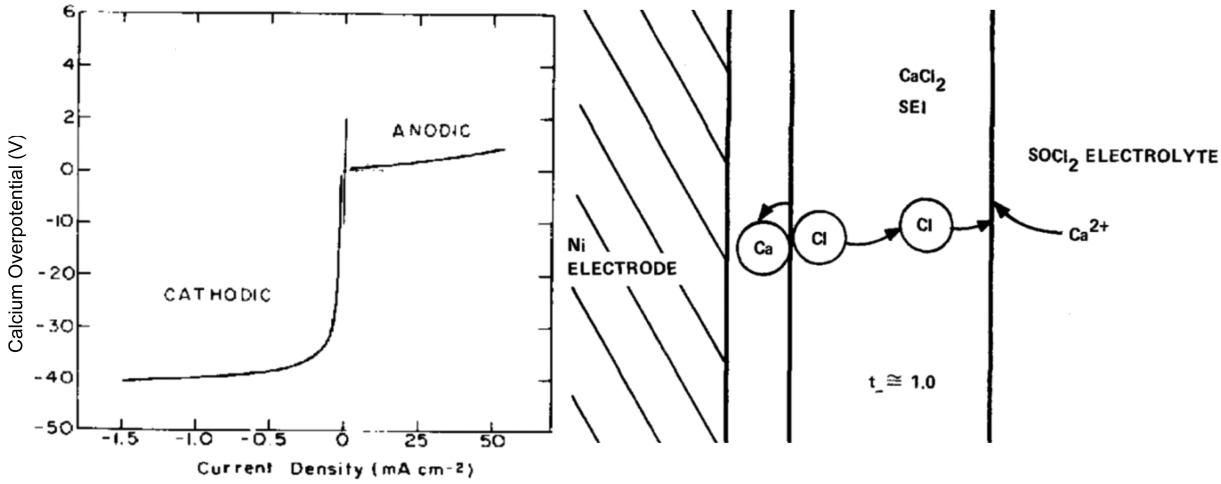

Figure 3. Left: *I*−*V* characteristics of a Ca^{2+}/Ca solid electrolyte interphase (SEI) covered electrode in a $SOCl_2$-based electrolyte (showing "diode-like" behavior). Reproduced from ref 25 with permission. Copyright [1988] Elsevier. Right: Model for calcium deposition through an SEI of $CaCl_2$. The ionic current is carried by the anion as a result of the low, close to 0, transport number of Ca^{2+}. Reproduced with permission from ref 21. Copyright [1980] The Electrochemical Society.

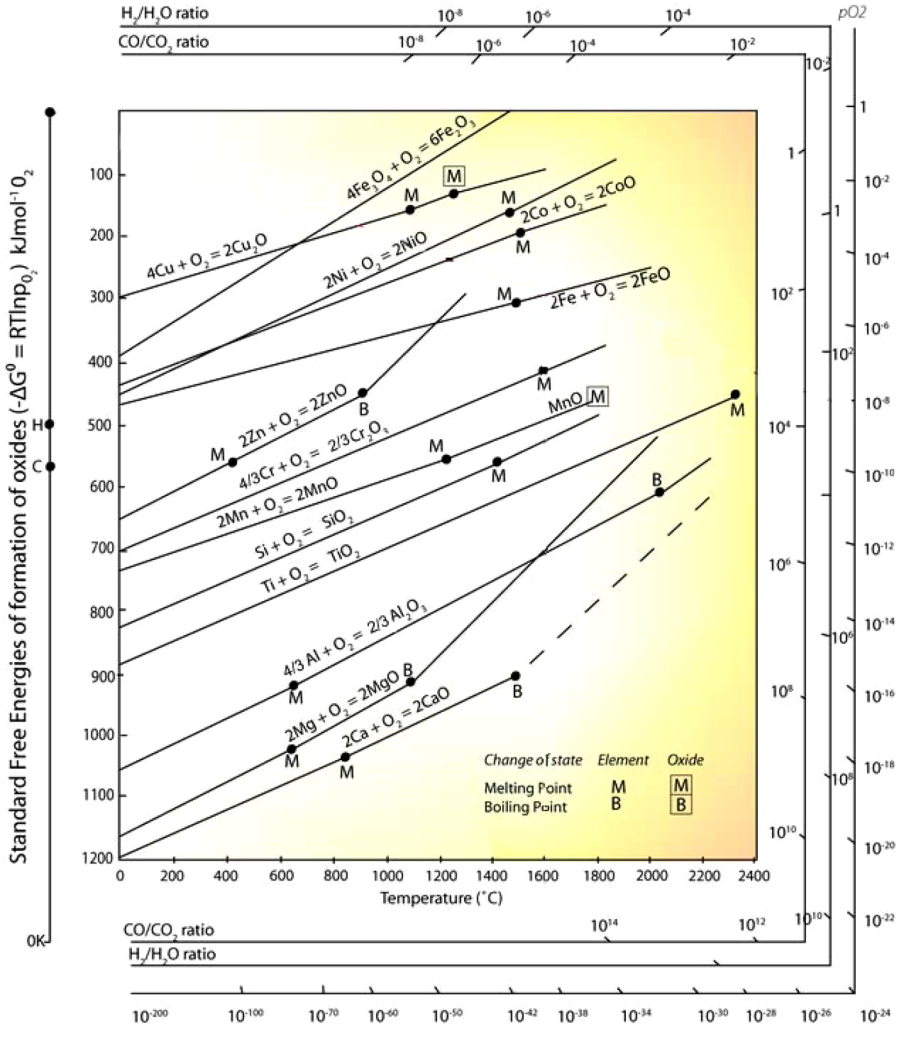

Figure 4. Ellingham−Richardson diagram of the standard free energy of formation for oxides vs temperature, together with the corresponding equilibrium O_2 partial pressure. Reproduced with permission from ref 72. Copyright [2018], University of Cambridge.

the larger size and charge of the Ca^{2+} ion as compared to the Li^+ ion, and to less extent to the Na^+ ion, for which many suitable hosts exist. To date, the cathodes proposed have been very few and are treated in detail in section 2.3 below.

DOI: 10.1021/acs.chemrev.9b00339
Chem. Rev. 2020, 120, 6331−6357

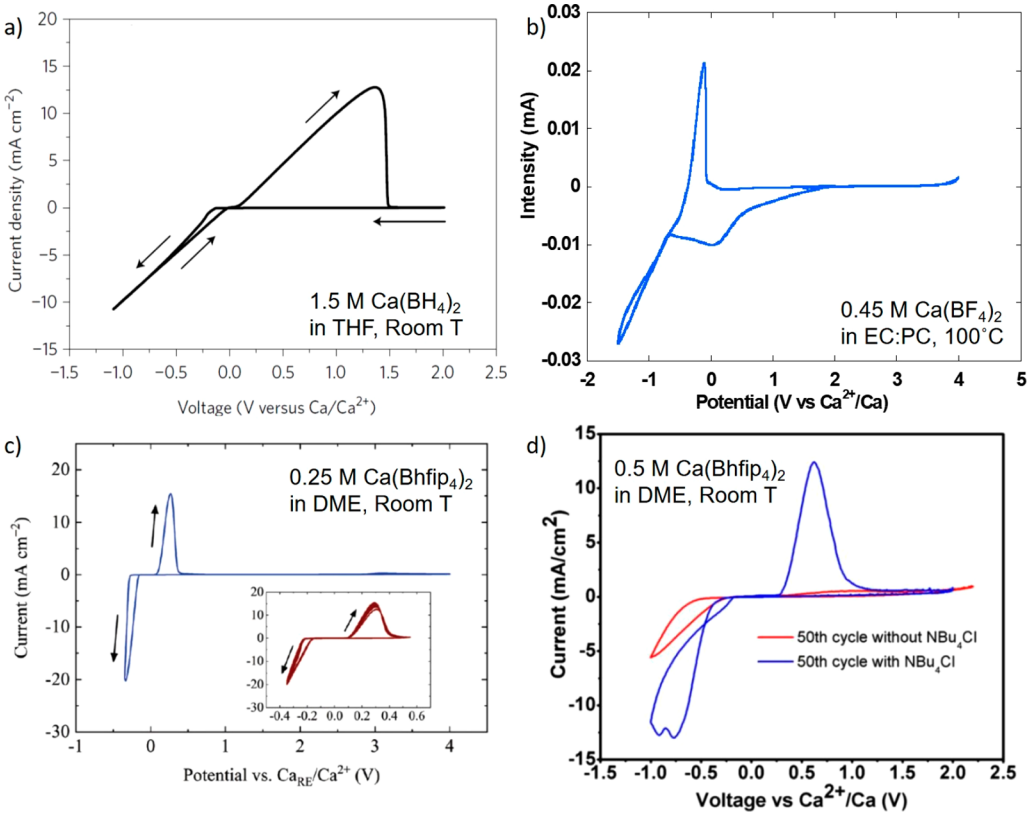

Figure 5. Cyclic voltammograms of calcium plating/stripping in (a) 1.5 M $Ca(BH_4)_2$ in THF (room temperature, 25 mV/s, working, reference, and counter electrodes Au, Ca, and Pt, respectively), reproduced from ref 73 with permission, copyright [2018] Nature Publishing Group, in (b) 0.45 M $Ca(BF_4)_2$ in EC:PC (100 °C, 0.5 mV/s, stainless steel working and Ca counter and reference electrodes), reproduced from ref 74 with permission, copyright [2016] Nature Publishing Group, in (c) 0.25 M $Ca[B(hfip)_4]_2$ in DME (room temperature, 80 mV/s, Pt working and Ca counter and reference electrodes), reproduced from ref 79 with permission, copyright [2019] The Royal Society of Chemistry, and in (d) 0.5 M $Ca[B(hfip)_4]_2$ in DME with or without 0.1 M NBu_4Cl (room temperature, 25 mV/s, Au working and Ca counter and reference electrodes), reproduced from ref 78 with permission, copyright [2019] American Chemical Society.

2. ANODES, ELECTROLYTES, AND CATHODES

The choice of active materials together with the electrolyte sets the theoretical limits in voltage and energy density but also affects the kinetics (power), life-length, safety, and so on. A special role is played by the *interfaces* and in many cases also the *interphases* formed between the electrolyte and the electrodes. While also current collectors and casing materials and so on affect the final product, these are covered in section 3 dealing with full-cell design, rather than in separate subsections here.

2.1. Anodes

Several Ca battery anodes have been electrochemically tested, either in three- or two-electrode cell configurations, this is to say, with or without a reference electrode distinct to the counter electrode (Table 1). While the description of cell configurations is exposed in section 3, this section focuses in the anode side, and for simplicity, the contents are organized into two subsections; section 2.1.1 covers Ca metal anodes with the related interfaces, and section 2.1.2 covers alloys, intercalation materials, and other alternatives.

2.1.1. Ca Metal Anodes and Interfaces. The use of Ca metal anodes requires reversible stripping (at discharge) and plating (at charge). Several unsuccessful attempts to electrodeposit divalent cations have demonstrated the large difficulties associated with trying to accomplish this.[65] Based on the studies of Auborn et al. and Behl et al. on electrolytes of inorganic Li salts, e.g., $LiBCl_4$, $LiAlCl_4$, and so on, in phosphorus oxychloride ($POCl_3$) and thionyl chloride ($SOCl_2$) vs Li metal anodes,[66,67] Peled et al.[68] and Staniewicz[21] reported on the electrochemical behavior of the M−$SOCl_2$ (M = Mg or Ca) electrolytes vs the corresponding metal anodes, with a cell reaction suggested to be analogous with the Li systems

$$2M + 2SOCl_2 \Leftrightarrow 2MCl_2 + SO_2 + S \quad (2)$$

In terms of specific energy density, the Ca−$SOCl_2$ cell reaction is ca. 300 Wh/kg (for sake of comparison, the Li system is ca. 700 Wh/kg). Although this technology was considered for the development of primary cells, efforts to electroplate Ca from $SOCl_2$-based electrolytes were made but failed. Indeed, while a high current density was recorded upon anodic polarization of a Ca metal electrode with relatively low overpotential (efficient stripping), a very high overpotential was recorded upon cathodic polarization (Figure 3), and solvent reduction led to SO_2 gas being formed. The Coulombic efficiency for the Ca plating reaction was estimated to be a mere 5%.[25] The low reversibility of the Ca plating/stripping reactions has in general mainly been attributed to the poor diffusion of divalent cations through the passivation layer formed (mostly $CaCl_2$) as well as its mixed ionic conductor nature, which precludes Ca plating (Figure 3). In contrast, Mg electrodeposition is possible, and the obtained deposit less prone to corrosion; a Ca deposit is completely consumed in less than 7 min after plating, whereas Mg electroplated on Ni appears to be stable for at least 2 h.[23,68]

DOI: 10.1021/acs.chemrev.9b00339
Chem. Rev. 2020, 120, 6331−6357

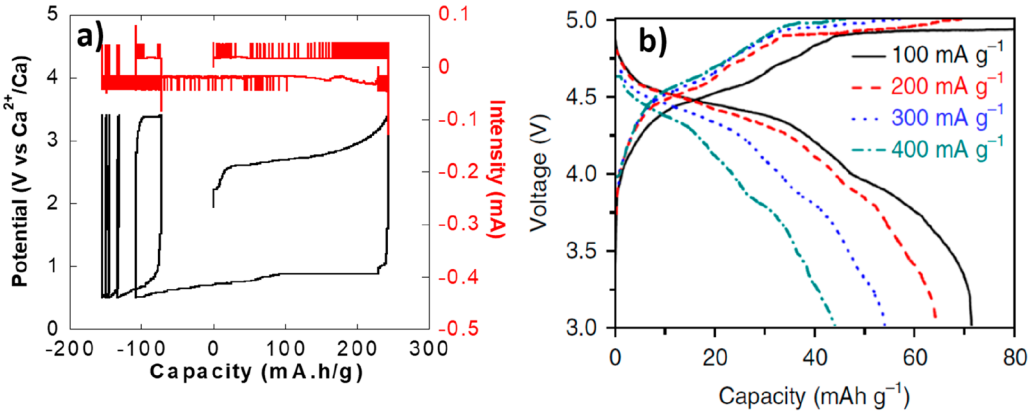

Figure 6. (a) Capacity vs potential profile from Potentiostatic Intermittent Titration Technique (PITT) of a $CaSi_2$ electrode at 100 °C. Reproduced from ref 58 with permission from Elsevier, copyright [2016]. (b) Charge−discharge performance of a Sn-expanded graphite Ca-ion cell at different current densities ranging from 100 to 400 mA g^{-1}. Reproduced from ref 82 with permission from the Nature Publishing Group, copyright [2018].

While the Ca metal anode is by far the most promising cell design, the electrochemistry of Ca metal is rather complex, including the role of the very stable calcium oxide. An Ellingham diagram[69] plots the standard free energy of formation of oxides with temperature, and it usually also provides the partial pressure of oxygen at equilibrium (Ellingham−Richarson diagram, as shown in Figure 4). The standard free energy is more negative for the more stable oxide; hence, CaO is clearly more stable than MgO and even Al_2O_3. The high stability of CaO is certainly a severe problem to overcome for those aiming at employing Ca−O_2 as the cathode. Since the entropy variation for the oxide formation is negative, the free energy becomes less negative as temperature increases. Therefore, it is not surprising that the first reports on Ca metal anodes in the early 1960s (section 1) were on cells operated at high temperatures (>450 °C).[13−15,17] The electrolyte chemistry was very similar to Ca metal production; molten salts, typically eutectic mixtures of $CaCl_2$ and CaF_2, were employed and involved electrowinning and electrorefining processes performed at >850 °C.[70] Later on, the concept of liquid metal electrodes also used higher temperatures, typically operating at >500 °C.[71]

Ca batteries are very much dependent on the properties and performance of the electrolyte/electrode interfaces. In an early study by Aurbach et al.,[32] the process of calcium plating at the anode from an organic electrolyte was explored using $Ca(BF_4)_2$ and $Ca(ClO_4)_2$ as the electrolyte salts and PC, gBL, THF, and ACN as the solvents. The plating was found by infrared spectroscopy to be limited by the electrolyte decomposing to form a passivation layer on top of the Ca metal, hence akin to the solid electrolyte interphase (SEI) formed on graphite in LIBs. In contrast to LIBs and why the term SEI should not be used here, among all the different electrolytes studied, none of them allowed for reversible plating/stripping of calcium, as the passivation films, mainly composed of $CaCO_3$ and $Ca(OH)_2$, did not conduct Ca^{2+} ions. Although these observations severely stalled the development of Ca metal-anode-based batteries, two recent studies have indeed reported on successful calcium plating and stripping using organic electrolytes in the presence of passivation layers: 1.5 M $Ca(BH_4)_2$ in THF[73] and 0.45 M $Ca(BF_4)_2$ in EC:PC.[74] The former electrolyte enables reversible cell performance at room temperature, with an electrochemical stability window of about 3 V, while the latter offers over 4 V but demands an elevated temperature (100 °C) (Figure 5). For $Ca(BH_4)_2$ in THF, the passivation layer was found to be entirely composed of CaH_2 formed by the reaction of Ca metal with the solvent. Unfortunately, the CaH_2 passivation layer was found to continuously grow upon cycling and is highly reactive. Recently, Ta et al. have performed a systematic fundamental study on the Ca plating mechanism using this electrolyte and a Au or Pt rotating disc electrode setup, suggesting a chemical−electrochemical deposition mechanism, with the kinetics of the chemical step (involving hydrogen adsorption) being substrate-dependent and faster with Pt than with Au.[75]

For the $Ca(BF_4)_2$ in EC:PC electrolyte-based cells, the situation is more complex; several solvent decomposition products were identified including CaF_2 and carboxylates but not which one(s) that enabled Ca migration.[74] Young et al. investigated possible reduction pathways for EC and $Ca(ClO_4)_2$ in EC (thus not the same anion as in the experiment) by means of DFT and AIMD simulations and concluded that $CaCO_3$, CaO, and $Ca(OH)_2$ should be the major inorganic components of the SEI.[76] Later on, a detailed study on the passivation layers formed from $Ca(BF_4)_2$ or $Ca(TFSI)_2$ in EC:PC electrolytes allowed calcium carbonates, fluorides, and borates to be identified—with the latter only being observed for BF_4^--based electrolytes, the electrolyte in which Ca plating and stripping is feasible, i.e., no plating is observed for the electrolyte containing TFSI.[77] Further experiments used an electrode prepassivation step by a BF_4^--based electrolyte. The prepassivation procedure consisted in polarizing a stainless steel current collector at low potential in order to produce a borate containing passivation layer. Subsequently, after a thorough rinsing procedure, the electrode was transferred to a cell with a TFSI containing electrolyte.[77] Thereby could not only Ca plating be observed, using the previously inactive $Ca(TFSI)_2$-based electrolyte, but also an enhanced electrochemical response—ca. 4 times higher current densities. This strongly suggests that the nature of the passivation layer is key to enable Ca plating and that the composition of the electrolyte plays a major role in the overall plating kinetics. Both the cation mobility in the electrolyte and interfacial phenomena such as desolvation are thus interconnected properties of utmost importance for practical Ca batteries.

In 2019, two independent studies demonstrated Ca plating and stripping at room temperature using Ca salts based on fluorinated alkoxyborate anions and dimethoxy ethane (DME) as solvent. Coulombic efficiencies between 80 and 90% were reported together with anodic stabilities above 4 V vs Ca^{2+}/Ca

DOI: 10.1021/acs.chemrev.9b00339
Chem. Rev. 2020, 120, 6331−6357

and the presence of CaF_2 as an electrolyte decomposition product.[78,79] These studies represent a significant step forward in the development of a room temperature Ca metal-anode-based battery and should be benchmarked against cathode materials. Nonetheless, the need for a conditioning protocol (five cyclic voltammetry cycles at 80 $mV{\cdot}s^{-1}$)[78] or addition of 0.1 M Bu_4NCl[79] in order to achieve the high Ca plating/stripping Coulombic efficiency or to improve cyclability also calls for additional work on surface passivation and in order to identify the electroactive species. The possibility/risk of Ca dendrite growth is also mentioned, as characteristic structures were observed growing through the separator, and a short circuit was recorded at a current density of 1 $mA.cm^{-2}$.[78]

2.1.2. Alloys, Intercalation Materials, and Other Alternatives. Alloys are considered a viable alternative to Ca metal anodes, as they often have both high specific capacity and low potential.[61,80] As expected from the divalent nature of Ca and Mg cations, a similar volume expansion can be calculated for the formation of A_xM (with A = Ca or Mg and M = Sn, Si, etc.) as for the formation of $Li_{2x}M$, and a similar amount of charge is stored.[61] Si- and Sn-based alloys investigated electrochemically showed decalciation of $CaSi_2$ to be possible using 0.45 M $Ca(BF_4)_2$ in EC:PC electrolyte at 100 °C, leading to an average particle diameter size decrease from 7.3 to 2.6 μm.[58] A large voltage hysteresis was, however, observed upon reduction, and amorphization prevented any confirmation of alloy reformation. Tang's group investigated a Sn anode using a 0.8 M $Ca(PF_6)_2$ in EC:PC:DMC:EMC (2:2:3:3 by vol.) electrolyte and a graphite cathode (employing anion insertion).[81,82] Since only two-electrode cells were assembled, the capacity vs voltage profile of Sn is not really unambiguously determined, but yet, a much smaller voltage hysteresis was obtained as compared with the Si anode (Figure 6). Even though 350 cycles were reported, the low Coulombic efficiency (ca. 80%) suggests a significant amount of parasitic reactions, most probably involving electrolyte decomposition. In addition, the $Ca(PF_6)_2$ salt employed is known to be quite unstable.[83]

A systematic screening and high-throughput density functional theory (DFT) investigation of a large number, in total 115, of Ca_xM alloys was very recently made by Wolverton's group.[80] The most promising alloy candidates were selected considering calciation voltage, volume expansion, and specific capacity. These criteria resulted in a wide range of metals being considered worthy of further investigation; M = Sn, Si, Sb, Ge, Al, Pb, Cu, Cd, $CdCu_2$, Ga, Bi, In, Tl, Hg, Ag, Au, Pt, and Pd. Pt and Au attract special interest, as these metals sometimes are used as substrates/working electrodes (Table 1), emphasizing that care must be taken to ensure that alloy formation does not bias the interpretation. Ca alloys were also considered in thermal batteries as a way to overcome the high melting point of Ca (842 °C). The operation temperature of such cells could be lower by using Ca alloys such as Ca−Bi,[48] Ca−Sb,[84] Ca−Ge,[85] and Ca−Mg.[47,51]

Not only simple metal alloys are advocated for; two-dimensional GeP_3 was recently investigated by DFT as a potential anode for several post-Li batteries,[86] Ca^{2+} was found to preferentially react with GeP_3 through a conversion reaction resulting in a theoretical specific capacity of 658 mAh/g.

Graphite is by far the most representative and studied insertion anode material for the LIB technology. While fellow alkali earth metals such as barium (Ba) and strontium (Sr) have been found to intercalate in graphite rather easily,[87] Ca intercalation using a similar procedure (contact of graphite with the metal vapor) only leads to superficial intercalation.[88] So far, only dimethyl sulfoxide (DMSO)-solvated Ca has been intercalated readily into graphite.[59] Successful preparation of CaC_6 was, however, claimed by Emery et al. after immersing graphite in a molten lithium−calcium alloy at 350 °C for 10 days.[59] The authors suggested that only Ca is intercalated and mentioned that the CaC_6 crystal structure is unique (rhombohedral and $R\bar{3}m$ space group) as compared to other MC_6 compounds having hexagonal symmetry. Wu et al. assembled a dual-carbon electrode cell using a *meso*-carbon microbead (MCMB) anode and an expanded graphite cathode.[89] Upon cycling, reversible shifts of the (002) graphite diffraction peak were observed as well as a broadening, showing loss in graphitization degree (Figure 7). Unfortunately, since all

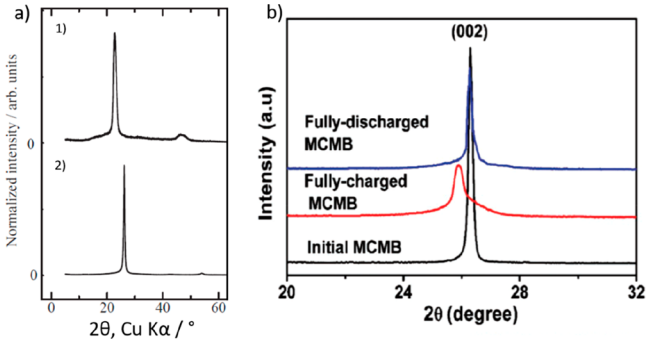

Figure 7. (a) XRD patterns of (1) Ca-intercalated BC_8 and (2) original BC_8 films. Reproduced from ref 90 with permission from The Chemical Society of Japan. Copyright [2018]. (b) XRD patterns of an initial, fully charged, and fully discharged MCMB anode in a Ca dual-carbon electrode battery (expanded graphite used as cathode) during the initial cycle. Reproduced from ref 89 with permission from Wiley-VCH. Copyright [2018].

tests were performed using two-electrode cells, no conclusions can be drawn with respect to the intrinsic performance and operating voltage of the MCMB anode. Ishikawa et al. proposed an interesting strategy for Ca insertion by first preparing BC_8,[90] which allowed for easier Ca intercalation using the standard method, something rationalized by the relationship between the ionization potential of Ca and the electron affinity of BC_8. Borophene, the boron analogue to graphene, and hydrogenated defective graphene, have both been investigated by DFT for possible application as Ca battery anode materials.[91,92] Higher binding energies were obtained for Ca than for Mg, Li, and Na, and specific capacities of 800 and 591 mAh/g were obtained, individually. Datta et al. investigated the adsorption of Ca (and Na) on graphene with divacancies and Stone−Wales defects[93] and concluded that adsorption is not possible on pristine graphene but enhanced by increasing the density of defects, with a calculated capacity of 2900 mAh/g for Ca^{2+} adsorption. As for every other high-surface-area anode material, however, it is very unlikely that graphene can be used in practice, as the side-reactions taking place would be highly detrimental and result in an excessive cation inventory loss. In addition, the low-density graphene-based anodes will result in low volumetric energy density cells. MXenes have also been considered as anodes for Ca, K, Na, and Li batteries.[94,95] By DFT calculations, the adsorption energies were found to decrease as the coverage increased, and a larger effective ionic radius was found to increase the interaction between the alkali and alkali earth atoms, penalizing the capacity; 320 mAh/g for Ca^{2+}. However,

DOI: 10.1021/acs.chemrev.9b00339
Chem. Rev. 2020, 120, 6331−6357

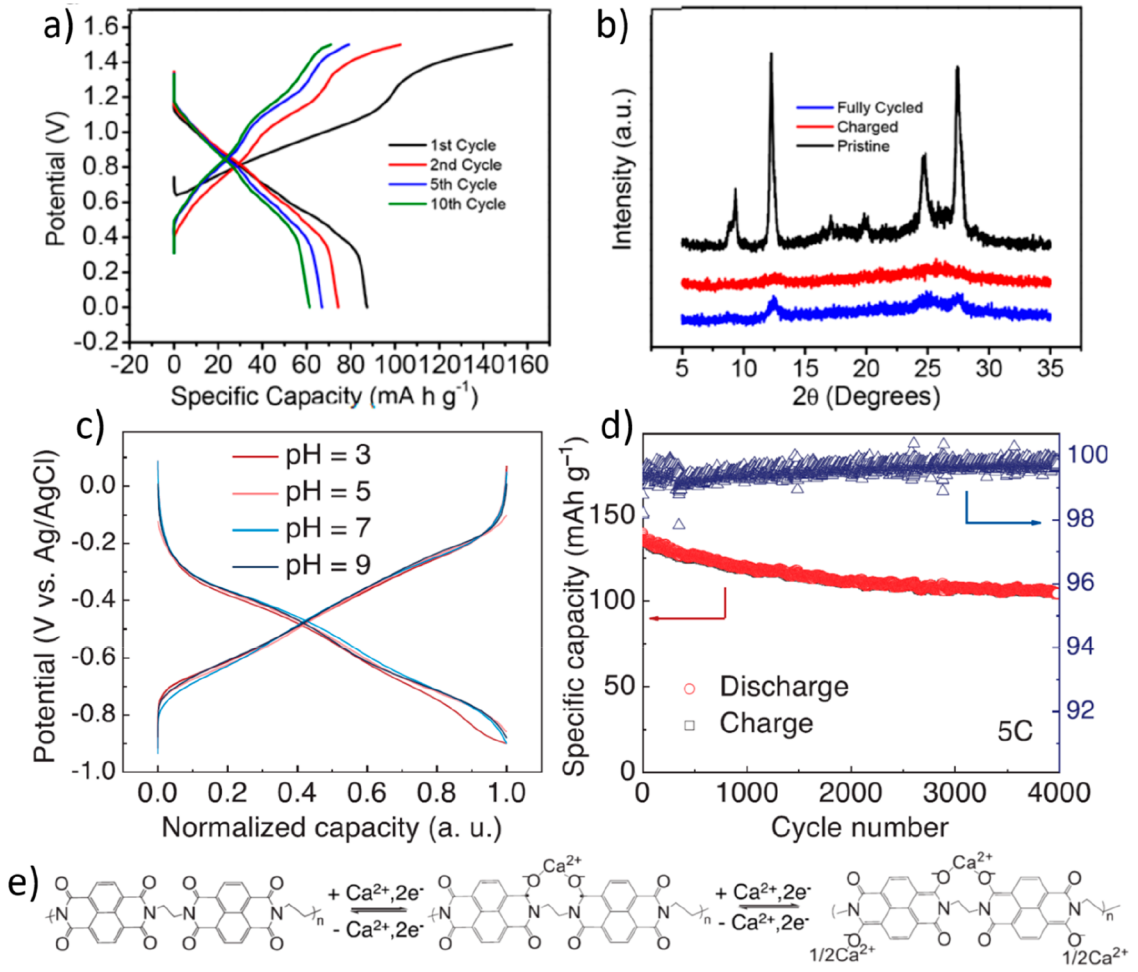

Figure 8. (a) Galvanostatic calciation/decalciation potential profiles of the PTCDA electrode in a two-electrode cell at a current density of 20 mA g^{-1}, and (b) ex situ XRD patterns of the PTCDA corresponding to the pristine (black), calciated (red), and decalciated (blue) electrode. Reproduced from ref 96 with permission from the American Chemical Society, copyright [2017]. (c) Charge−discharge profile of PNDIE electrodes in 2.5 M $Ca(NO_3)_2$ aqueous electrolytes with different pH. (d) Capacity stability and Coulombic efficiency of PNDIE at 5C rate (925 mA g^{-1}). (e) Possible reversible electrochemical redox mechanism of PNDIE. Reproduced from ref 97 with permission from Wiley-VCH, copyright [2017].

MXenes have the common problem of all high-surface-area anode materials: poor first cycle Coulombic efficiency, i.e., a large irreversible loss of capacity.

Organic compounds have also been tested as Ca battery anodes using aqueous electrolytes (Table 1). The aromatic molecular solid 3,4,9,10-perylenetetracarboxylic dianhydride (PTCDA) was tested in a three-electrode cell using activated carbon as the cathode.[96] Despite some signatures of reversible electrochemical activity, XRD studies indicated rapid deterioration/amorphization upon cycling (Figure 8a,b), which was attributed to the large size of Ca^{2+}, as this behavior was not observed for Mg^{2+}. For a polyimide (PNDIE) anode and a copper hexacyanoferrate cathode cell, a stable discharge capacity of 40 mAh/g (at C/10 rate) was demonstrated for 1000 cycles[97] This cycling was, however, performed at a 5C rate, thus potentially masking parasitic reactions/active material dissolution issues. Moreover, for most tests using aqueous electrolytes, the issue of reactivity of protons as well as the role(s) of the oxygen reduction and/or the hydrogen evolution reactions, ORR and HER, respectively, is rarely mentioned, even though the voltage window commonly explored is >1.4 V.

2.2. Electrolytes

Regardless of battery design and concept, the role of the electrolyte is primarily to efficiently separate the two electrodes, which is in practice solved by some kind of membrane/separator layout, and to efficiently transport the ionic charge carrier(s) of interest between the electrodes.[99] Due to the (very) hard acid−base nature of both the Mg^{2+} and Al^{3+} cations, the corresponding multivalent-battery technologies have very special electrolyte compositions to enable desolvation of the cations at the electrode/electrolyte interfaces—especially because the solvents are very cumbersome to create and handle.[8] In contrast, Ca battery electrolytes are much more similar to both LIB and SIB electrolytes, and simple salt-in-solvent concepts using standard battery solvents from these technologies seem to provide the needed overall bulk electrolytes properties—likely beause Ca^{2+} is a much softer cation. The remaining open questions are mainly related to if these suffice to provide ample Ca^{2+} transport and exchange at the electrodes.

While Ca battery electrolytes basically must only fulfill the condition of fast and large enough Ca^{2+}-ion transport, through the bulk and at the interfaces, to not limit the power performance of the cell—and in some cases make it at all cyclable—there is the additional issue of enough (electro-)

DOI: 10.1021/acs.chemrev.9b00339
Chem. Rev. 2020, 120, 6331−6357

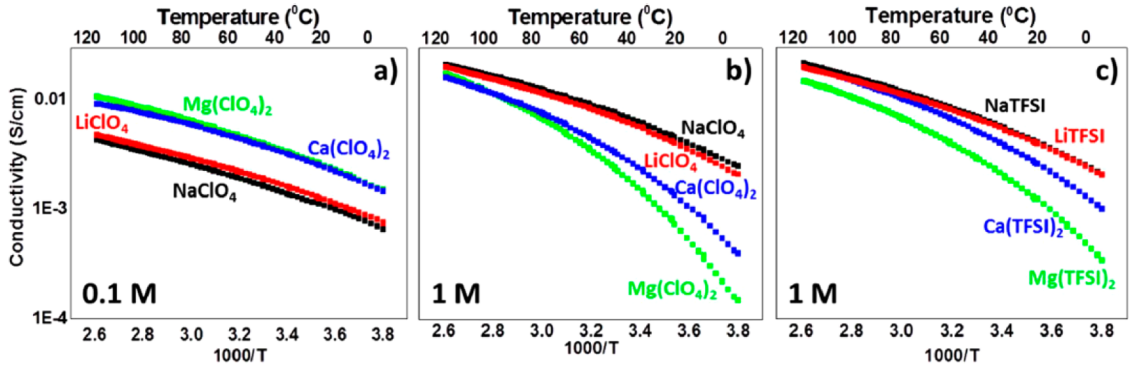

Figure 9. Arrhenius plots (between −10 and 120 °C) for various Li/Na/Ca and Mg salts in $EC_{0.5}$:$PC_{0.5}$ with (a) 0.1 M and (b,c) 1 M salt concentrations. Reproduced from ref 101 with permission from The Electrochemical Society, copyright [2017].

chemical stability. This is due to the electrochemical potential of Ca being so low and close to Li. From the perspective of electrolyte and anode compatibility, basically the cathodic stability of the salt anion(s) and the solvent(s) used, two main approaches have been employed:

(i) electrolytes that form a passivation layer on Ca metal anodes by limited decomposition of salt and/or solvents, i.e., are metastable. The main issue is then Ca^{2+} mobility through the passivation layer;

(ii) electrolytes that do not form any passivation layer—thus being intrinsically stable, primarily suited for nonmetallic anodes, rendering cells with lower energy density.

From the electrolyte vs cathode perspective, both electrolyte designs above hitherto often have rather limited electrochemical stability windows (ESWs), in principle hindering the use of really high-voltage cathodes—but at the same time no practical Ca cathodes (see section 2.3) exist to date.

A major limitation common to all Ca battery electrolytes is the limited number of Ca salts commercially available. Most work has so far employed one or more of these five simple Ca salts: calcium perchlorate, $Ca(ClO_4)_2$, calcium tetrafluoroborate, $Ca(BF_4)_2$, calcium bis(trifluoromethanesulfonyl)imide, $Ca(TFSI)_2$, calcium nitrate, $Ca(NO_3)_2$, and calcium borohydride, $Ca(BH_4)_2$. As the ClO_4^- anion is laden with safety issues, the latter four salts are strongly recommended for any practical studies. For aqueous electrolytes, the salt of choice has distinctively been $Ca(NO_3)_2$. Up to now, there has been no systematic investigation on the impact of the nature of the salt in divalent-cation aqueous systems; the choice of nitrate salt most probably is rooted in historical reasons.

In 2015, however, Lipson et al.[100] reported on the synthesis of calcium hexafluorophosphate, $Ca(PF_6)_2$, salt, and furthermore, in 2017, Keyzer et al.[83] showed a direct anhydrous synthesis route for the same salt—something they previously developed for the Mg analogue. The latter study is particular significant, as it makes quite an effort targeting the chemical stability of the PF_6^- anion—noting that the chemically softer Ca^{2+} (as compared to Mg^{2+}) would have a weaker solvent interaction and thereby accelerate the anion decomposition by stronger cation−anion interaction, i.e., ion-pairing. However, the latter is also weakened by the cation being softer, and to us, it is not clear what interaction is affected the most: cation−solvent or cation−anion, calling for computational and spectroscopic local interaction studies. The synthesis is also significant given that the PF_6^- anion is part of the standard LIB electrolyte design, stressing further possibilities to create Ca battery electrolytes using LIB know-how but with the difference that the anion must comply with cycling vs Ca metal anodes.

Apart from water as the solvent for aqueous electrolytes, more or less standard LIB solvents such as THF, ACN, gBL, PC, DMC, DEC, EMC, DMF, dimethoxyethane (DME), and mixtures of EC and PC have all been applied as matrices for the above Ca salts—even if not all possible combinations. The crucial feature of the metastable electrolytes according to (i) above is that the degradation products arise electrochemically by reduction, often due both to solvent and salt anion, creating a covering and stable film onto the anode, i.e., an SEI. These electrolytes and the truly stable ones are discussed further in section 2.2.1.

In addition to the standard salt-in-solvent design, there are designs relying on ionic liquids (ILs) as solvents and also a few solid-state electrolytes (SSEs), ceramics, and polymers, which we briefly touch upon in section 2.2.2.

Below, the studies centering on Ca conducting electrolytes so far are summarized briefly, but many general Ca battery studies simply use one or two electrolytes without any motivation and from this extrapolate/generalize. We would therefore like to stress that for further development, there is a need for work with the electrolyte in focus to enable:

(i) a better understanding of the reactions at the interfaces—to tailor the SEI (if any),

(ii) a large mapping of salt(s), solvent(s), concentration(s), and additives and how these alter densities, viscosities, conductivities, ESWs, Ca^{2+} transport, etc.,

(iii) a use of more LIB and SIB electrolyte know-how as well as from Mg and Al batteries.

2.2.1. Liquid Electrolytes. Nonaqueous organic-solvent-based liquid electrolytes have by far been the prevailing choice for Ca batteries, even if aqueous electrolytes have been shown to improve the kinetics of Ca intercalation at the electrolyte/electrode interface. Systematic electrolyte studies are hitherto very scarce. We note the early "screening" study by Aurbach et al.[32] investigating the electrochemical behavior of a Ca metal anode in different organic electrolytes composed of ACN, THF, gBL, and PC and the salts $Ca(ClO_4)_2$ and $Ca(BF_4)_2$ and the similar study by Hayashi et al.[42] using $Ca(ClO_4)_2$ as the salt and PC, DMC, DEC, EMC, gBL, DMF, and ACN as solvents. In contrast, most often a single or at most two different electrolytes have been employed to study an anode or cathode in half- or full-cell designs. The three most prominent examples are the studies on reversible Ca plating and stripping using a Ca metal anode by Ponrouch et al.[74] using different Ca salts in EC:PC, by Wang et

DOI: 10.1021/acs.chemrev.9b00339
Chem. Rev. 2020, 120, 6331−6357

al.[73] employing $Ca(BH_4)_2$ in THF, and by the groups of Nazar[78] and Fichtner[79] using Ca salt based on fluorinated alkoxyborates anions in DME. These studies are covered extensively in section 2.1 with respect to the functionality for the anode and interface creation. We note here, however, that these research groups used different salt concentrations—with 0.25 M $Ca[B(hfip)_4]_2$, 0.45 M $Ca(BF_4)_2$, 0.5 M $Ca[B(hfip)_4]_2$, or 1.5 M $Ca(BH_4)_2$—a far from small design difference and significant for the electrolyte properties. Another note is that these electrolytes have a fair concentration of oxygen atoms by virtue of the carbonate solvents, and combined with the stability of the CaO (Figure 4), this might have profound effects on the cyclability of Ca-metal-based cells (see section section 2.1, Figure 5).

In a recent study, the Ca salt type and concentration was systematically varied in a matrix of EC:PC.[101] The target was truly electrolyte oriented to connect various fundamental physicochemical electrolyte properties such as ion conductivity, viscosity, and the Ca^{2+} cation solvation by solvent and anions, with the practical electrochemical performance. It also compared Ca^{2+} vs Li^+, Na^+, and Mg^{2+} in order to strengthen the fundamental understanding of the importance of underlying interactions for the phenomena and correlations observed. It was deduced that for low salt concentrations (0.1 M), when almost total ion−ion dissociation can be expected, the divalent systems are *more* conductive than the corresponding monovalent-cation-based systems, while for higher concentrations (1.0 M), both the viscosity and the ion-pairing increases relatively more for the divalent systems, and consequently, the ion conductivity drops (Figure 9). At elevated temperatures, such as those used to enable the reversible stripping/plating in the former studies, however, these differences become less obvious (Figure 9b,c). Also, the nature of the anions matters—employing the TFSI salt renders more conductive electrolytes for the 1.0 M system (Figure 9b,c)—primarily by less extensive ion-pairing.

The ionic conductivities were all above the target value often given for LIB electrolytes (1 mS/cm): ca. 3.5 mS/cm even at room temperature for the 0.1 M systems and slightly lower, ca. 2.0−2.8 mS/cm for the 1.0 M systems. The differences correlate with the viscosity of ca. 3 cP increasing to a vast 70 cP, which again can be mitigated by raising the temperature (Figure 10).

At a molecular level, the differences, especially with respect to the ion-pairing, can be analyzed by vibrational spectroscopy, showing that the cation solvation numbers are lowered from 6.7 to 5.3 from 0.1 to 1.0 M $Ca(TFSI)_2$ concentration but also that Ca^{2+} has a larger first solvation shell than all other cations (Li/Na/K/Mg).[32] This should affect the mobility in the bulk as well as the (de)solvation dynamics at the electrolyte/electrode interfaces.

A note of caution is also needed with respect to the discussion of ion conductivities above; a 0.1 M $M(TFSI)_2$ electrolyte has nominally 50% more ions than a 0.1 M MTFSI electrolyte. Hence, analysis of (cation) transference numbers and not only the total ion conductivities is crucial.

Comparing the above systems, the EC/PC-based electrolytes exhibit a 4 V ESW and are thus in principle suited for medium−high-voltage cathode materials, while the THF-based electrolyte is more limited (<3 V).

Turning to water, real aqueous electrolytes as well as water present in conventional aprotic electrolytes have been shown to stimulate formation of a calcium hydroxide film passivating a Ca metal anode.[32] Hexacyanoferrates were used as cathodes in the

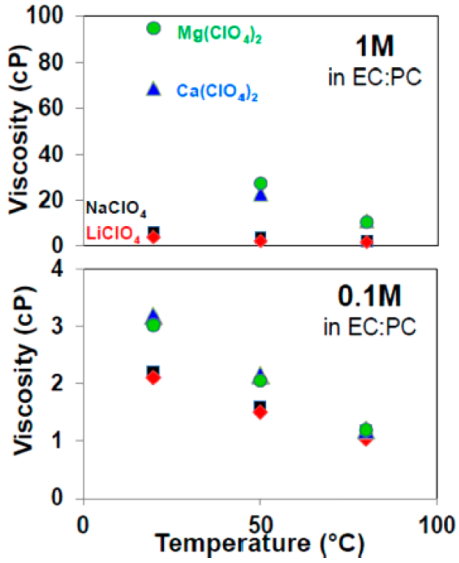

Figure 10. Viscosities for $Ca(ClO_4)_2$ in EC:PC electrolytes for the two salt concentrations (0.1 and 1.0 M) as a function of temperature. Reproduced from ref 32 with permission from the The Electrochemical Society, copyright [1991].

early 2000s,[40] and more recently, this system has been reinvestigated,[41] also using nonaqueous electrolytes,[52] showing both a very reversible electrochemical response and enhanced capacity from the water addition. As an example, ca. 17% of water in a $Ca(ClO_4)_2$ in ACN electrolyte led to enhanced redox activity, attributed to solvation effects.[53] The role of water in the electrolytes for the intercalation is not fully elucidated—some studies point to minor changes in the host.[55] We caution for other events such as proton intercalation,[102] electrolyte decomposition, and/or current collector corrosion, which all can lead to misleading conclusions/assumptions with respect to calcium intercalation.

Protic electrolytes have also been employed for Ca−O_2 batteries, but to reduce the reactivity of Ca with water, a solvent mixture of 2:1 methanol:water without any Ca salt inside was employed—as its role is more to transport O_2 to the anode[103] than to transport any Ca^{2+}.

A bit more fundamental aqueous electrolyte properties were partly investigated by Wang et al.[41] using 1 M $Ca(NO_3)_2$ as salt. The target was fast migration of Ca^{2+} in electrodes, but Lee et al. showed more elaborately that highly concentrated aqueous electrolytes, also known as water-in-salt electrolytes (WISEs),[104] are also possible for Ca^{2+}.[105] The lowered hydration number, by increasing the $Ca(NO_3)_2$ concentration and thereby a greater amount of anions coordinating the cation,[105,106] diminished the activation barrier for intercalation, leading to improved cell cycling performance.

For all the above aqueous electrolytes, the issue of CaO formation, in contrast to the carbonate-based nonaqueous electrolytes, is a nonissue, as cells are not targeting Ca metal anodes.

2.2.2. Other Concepts. As well as there are few modern studies of alternative Ca battery concepts, the same is true for the electrolytes employed (disregarding the molten salt electrolytes covered extensively in section 1.1). Yet, application of solid-state electrolytes (SSEs)[84] and ionic-liquid (IL)-based electrolytes[63] has been given some minor attention.

DOI: 10.1021/acs.chemrev.9b00339
Chem. Rev. 2020, 120, 6331−6357

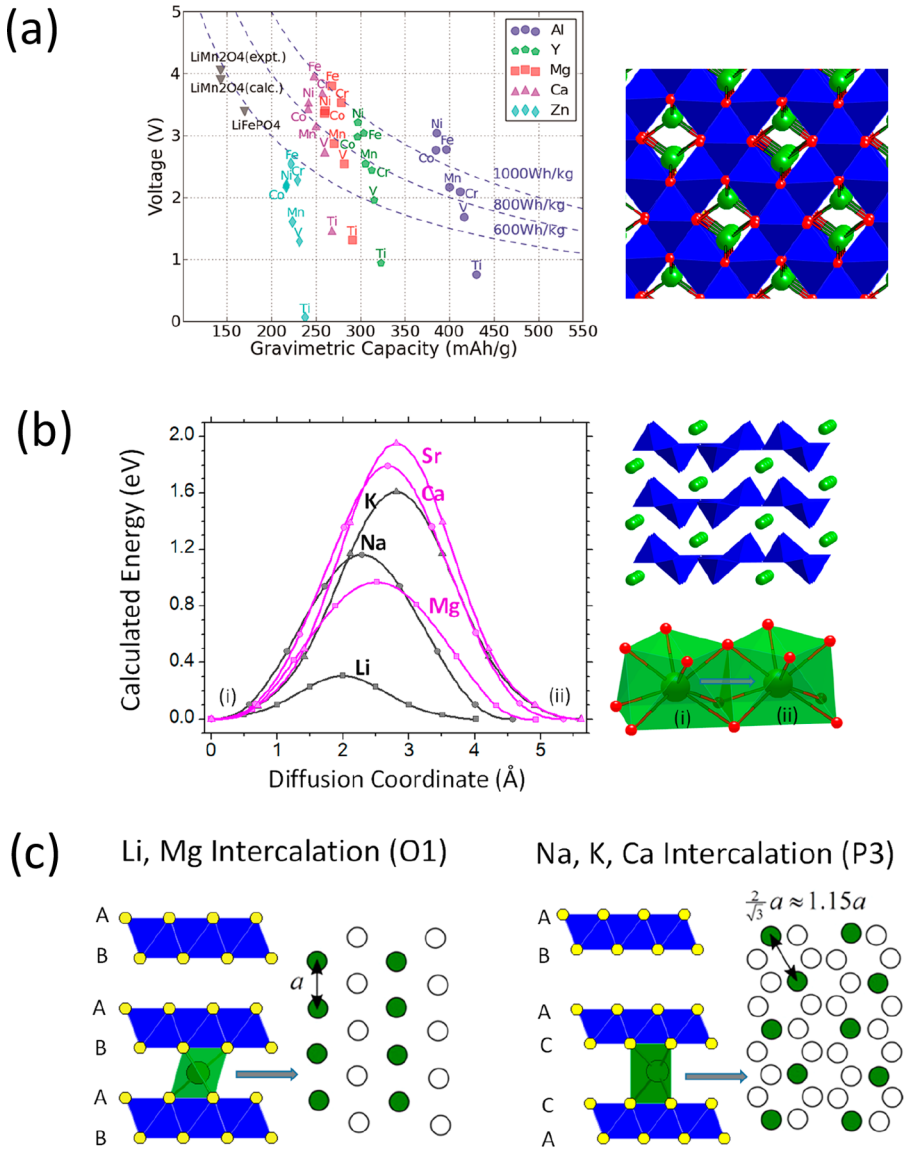

Figure 11. Some Ca^{2+} (comparative) intercalation electrode properties calculated by DFT: (a) intercalation voltage vs specific capacity in spinel-$Ca_T[M_2]_OO_4$, reproduced with permission from ref 57, copyright [2015] The Royal Society of Chemistry. The right panel shows the spinel structure. Color code: O in red, TM in blue, and Ca in green. (b) Diffusion barriers in $A_xV_2O_5$ for A = alkali or alkali earth cation, adapted with permission from ref 123, copyright [2014] American Chemical Society. The right panel shows the structure of V_2O_5 with potential sites for Ca insertion and the two sites (i) and (ii) involved in the Ca hop. Color code: O in red, TM in blue, and Ca in green. (c) The most stable $A_{0.5}TiS_2$ structures for A = Li, Mg, Na, K, and Ca. Color code: S in yellow, TM in blue, and Ca in green. Reproduced with permission from ref 128, copyright [2016] American Chemical Society.

Starting with the latter, the high ionic mobility, large ESWs, and great solubility power and safety trends—low or no vapor pressure—of ILs have attracted the attention of the battery community at large as electrolyte solvents. For Ca batteries, however, we know only of one single study, wherein Shiga et al.[63] investigated a nonaqueous $Ca-O_2$ battery design employing 0.1 M $Ca(TFSI)_2$ in the IL DEME TFSI and observed Ca plating/stripping at 60 °C. The CV indicates only a slightly reversible deposition of Ca, and the SEI formed was by Raman spectroscopy revealed to have a composition characteristic of TFSI anion decomposition.

Turning to SSEs, solid CaF_2 was used early vs alloys such as Ca−Bi and Ca−Sb.[84,107] Much more recently, metal borohydride electrolytes were investigated by DFT calculations, but in a comparative study, the Ca^{2+} diffusion was predicted to be too slow for practical application.[108] Overall, very few papers have reported on Ca^{2+} SSEs—despite the current "hype" on ASSBs, likely due to the difficulty to obtain materials with high-enough ionic mobility for this multivalent chemistry.

Solid polymer electrolytes (SPEs) containing Ca have been until now reported at the materials level but not with any real battery tests, including an early work almost 25 years ago using "home-made"(!) $Ca(TFSI)_2$ dissolved in a poly(ethylene oxide) matrix investigating basic properties such as cation coordination, ion conductivity, phase transformations, and so on.[109] We are aware that continued research on SPEs has been pursued in several laboratories since then but with no results in the open literature. A deviation from the SPE concept is gel polymer electrolytes (GPEs), and very recently, a Ca conducting GPE based on $Ca(NO_3)_2$ and a PEGDA cross-linked network was presented.[110]

DOI: 10.1021/acs.chemrev.9b00339
Chem. Rev. 2020, 120, 6331−6357

2.3. Cathodes

As only a few Ca battery cathodes have been successfully tested electrochemically, this section follows a different layout than for the anode and electrolyte, and it also emphasizes the role of computational studies. Section 2.3.1 analyzes the relation between intercalation and crystal chemistry, which is the base for Ca-cathode identification/design. The following subsections discuss targeted cathode properties: the energy density, which is maximized by increasing both the electrochemical capacity and the operation potential (section 2.3.2), and the practical power rates which depend, among other factors, on the Ca mobility in the cathode (section 2.3.3). Finally, alternatives to intercalation materials are presented in (section 2.3.4).

2.3.1. Intercalation and Crystal Chemistry. Intercalation, i.e., reversible insertion into a host with minimal structural change, is possible for a variety of electrochemically relevant metal ions (35,36,41,111−113). The basic requirements are an open framework of interconnected sites wherein the intercalated ion can diffuse and an electronic band structure able to reversibly accept/donate electrons.[114−118] The high redox potential needed to enable high cell voltages limits the suitable host materials to transition-metal (TM) containing compounds, just as for LIBs. The quest for cathode materials often relies on chemical intuition, and then, attempts are done to locate trends for a given host and different intercalated ions (44,56,57,101,112,119−128). Computational studies have been particularly important, since DFT permits the exploration of both existing and virtual materials, i.e., materials not (yet) made experimentally.[129,130] DFT (comparative) studies of Ca^{2+} include intercalation voltages (57,121−123,131−133) (Figure 11a), migration barriers (56,57,120,123,133) (Figure 11b), and phase stability (Figure 11c).[120,122,128,134] These studies uncover that trends are not straightforward. For Ca^{2+}, its divalent charge promises similarities with Mg^{2+} intercalation chemistry but is also alike Na^+ in size (ionic radii in metal oxides: $r(Ca^{2+})_{VI}$ = 1.0 Å and $r(Na^+)_{VI}$ = 0.99 Å[135]), resulting in similar site preference. Is then Ca intercalation reminiscent of Mg and/or Na intercalation? A plausible answer is that each metal is unique, and accordingly, the suitable host materials may be substantially different from one metal ion to other. The relation of intercalation to crystal chemistry is essential to identify possible cathode host materials and can be further analyzed looking at the host materials used as today's commercial LIB cathodes: olivine-$LiFePO_4$, spinel-$LiMn_2O_4$, and layered-$LiCoO_2$ (115,117,136,137).

In spinel-$LiMn_2O_4$ (Figure 11a), the Mn_2O_4 framework of edge-sharing octahedra provides a three-dimensional network of interconnected tetrahedral sites where the Li ion is located and can diffuse.[138] DFT investigations of virtual spinels $Ca_T[M_2]_OO_4$ (Ca in tetrahedral coordination) predicted some promising cathode properties (Figure 11a),[57] but yet, the preference of Ca ions for larger sites makes the preparation of such compounds very unlikely. Indeed, the $CaMn_2O_4$ stable polymorph—0.9 eV more stable than the spinel—is the marokite with Ca in 8-fold coordination sites.[134,139] While there are a few nitrides with Ca in tetrahedral coordination,[140] CaNiN[141] and Ca_3N_2,[142] the Inorganic Crystal Structural Database (ICSD) does not include any oxides with Ca in tetrahedral sites, and the ionic radii of tetrahedral Ca are not even listed for halides, chalcogenides,[143] or oxides.[135] Metastable structures with tetrahedral Ca could, however, be attempted by soft chemistry routes such as cation exchange, solvothermal, coprecipitation, or sol−gel processes, but even if $Ca_T[M_2]_OO_4$ spinels could be prepared, prolonged battery cycling might promote the thermodynamically stable structure, as previously observed for Mg spinels.[144−147] Site preference is certainly a prime difference between the intercalation chemistry of the larger Ca^{2+}, Na^+, or K^+ ions and the smaller Li^+ or Mg^{2+} ions, which is also influenced by their charge.

Turning to the olivine $LiFePO_4$, its hexagonal close-packing of oxygen has two different octahedral sites, M1 and M2,[148] where only the former provides channels for Ca diffusion.[149150] The M1 octahedron geometry is comparatively more distorted and smaller, whereas the M2 octahedron is more regular and larger. In $LiFePO_4$, the Li^+ ions occupy the smaller M1 site, and the Fe^{2+} cations occupy the M2 site. In olivine-$MgFeSiO_4$ and $MgMnSiO_4$, some degree of cation mixing is observed,[151,152] because of the similarity in the radii and equal charge of the two cations. In Ca olivines, however, as in the mineral kirschsteinite $CaFeSiO_4$,[153] the larger Ca^{2+} occupies the M2 site and is thus immobile.[154] The radii and the oxidation state of the intercalant and the TM ions combined regulate the cation distribution[155] and thus the suitability of given the structural type to intercalate different metals.

The structure of O3-$LiCoO_2$ (α-$NaFeO_2$ structural type) can be viewed as "ordered rock salt", in which layers of octahedrally coordinated Li^+ and Co^{3+} ions alternate within the cubic close packed oxygen array. The lithium ions can be reversibly removed from and reinserted within the triangular lattice of sites formed by the Li ions in a plane.[156−158] Like Li, Na combines with trivalent TM to form ordered rock-salt type structures with potential application as cathode materials in Na batteries.[159,160] In contrast, Ca^{2+} and TM ions preferably crystallize in structural types such as perovskites, postspinels, K_4CdCl_6, and so on, and due to cation distribution rules, few ordered rock-salt structures have been achieved: nanoclusters of $CaMnO_2$ superstructures[161] and layered-$Ca_{0.47}CoO_2$.[162] Cabello et al. prepared the latter metastable phase (see ref 163 for phase stability in the Ca−Co−O system) by the Pechini method[164] and reported a reversible capacity of ca. 30−100 mAh/g$CaCo_2O_4$ for 30 cycles, but deeper structural characterization is required to determine the Ca and Co distribution and its effect on the (low) capacity and cycling stability.[165−167]

Other crystal chemistries to analyze are the "traditional" insertion host materials, such as V_2O_5, MoO_3, and TiS_2,[36,168,169] that were explored long ago and found to exhibit a rich intercalation chemistry for a variety of intercalants. These materials have been extensively studied for Ca—especially V_2O_5,[35,43,125,170] a material that intercalates Li,[171] Na,[172] and even K.[173] Under ambient conditions, V_2O_5 crystallizes in a layered structure consisting of VO_5-square pyramids sharing edges and corners (Figure 11b). As layered structures favor intercalation reactions and the appealing high redox potential of the V^{5+}/V^{4+} couple, V_2O_5 was one of the first materials tested for Ca intercalation. Pioneering work by Amatucci et al.[35] reported a reversible capacity of 465 mAh/g for V_2O_5/PC nanocomposites,[44] further studied by Hayashi et al.[42,43] However, DFT investigations suggest a more sluggish kinetics for Ca intercalation than for Li, Na, and even Mg[120,123] (Figure 11b and section 2.3.3), and experiments show formation of protonated phases (section 3).[125,170] Another classical material in intercalation chemistry, TiS_2,[168,174,175] is among the very few compounds for which reversible Ca intercalation has been reported.[124,176] Recent DFT investigations indicate that distinct site preference of the intercalant ions drives the intercalation reaction in TiS_2 across different intermediate A_xTiS_2 phases

DOI: 10.1021/acs.chemrev.9b00339
Chem. Rev. 2020, 120, 6331−6357

(Figure 11c).[128] Thus, Mg and Li occupy the empty octahedral sites in the interlayer space of the initial O1 lattice (CdI_2-type structure), forming stage compounds as intercalation proceeds. In contrast, the large intercalants Na, K, and Ca occupy the prismatic sites in a P3 stacking (Figure 11c) at intermediate concentrations ($x \approx 0.5$), as this intercalant site topology minimizes the in-plane electrostatic repulsions.[128,177,178]

Hence, attempting to accomplish Ca battery cathode design with a large amount of parallelism between Ca and better known intercalation chemistries (Li, Na, or even Mg) is not really possible, as the crystal chemical analogies are too intricate.

2.3.2. Energy Density: Voltages and Capacities. In an insertion reaction, the intercalated ions are incorporated in the crystalline structure of the host compound, and electrons are added to its band structure. In a simplified model,[169,174,179] the intercalant metal ions are fully oxidized, donating electrons to the unoccupied levels of the band structure of the host compound, which arise from the antibonding d-states of the TM. Thus, the nature and the oxidation state of the transition-metal ion are the main determinants of the intercalation voltage, which depends also on the ionocovalent character of the cation−anion bond, primarily driven by the nature of the anion and in a lesser extent by the crystal structure.[169,179,180] In short, the Ca intercalation voltage for a given TM redox couple should follow the trend known from Li-cathode intercalation materials: chalcogenides < oxides < poly-oxoanionic.[136,179,181]

As there is so far very limited experimental data on Ca intercalation voltages available, DFT calculations have been extensively used to predict average values for several prospective materials (57,119,121,124,131−134,147,182). In a first step, the voltage is usually calculated between the fully intercalated and deintercalated compounds; this is $x = 0, 1$ in Ca_xTiS_2,[183] $x = 0, 2$ in $Ca_2Fe_2O_5$,[184] $x = 0, 3$ in $Ca_3Cr_2(SiO_4)_3$,[154] and so forth. While some oxidation states assumed might not be realistic—as the Mn^{7+} of fully deinserted $Ca_3Mn_2O_7$ and $Ca_4Mn_2O_7$[133]—this gives a fast overview of voltage trends. Subsequently, the average intercalation voltages for any intermediate compositions can be calculated using structural models of ordered calcium/vacancy arrangements, as has been done for instance in the perovskites Ca_xMO_3[132] or the Chevrel phase $Ca_xMo_6S_8$.[182]

The DFT-predicted Ca^{2+} average intercalation voltages for oxides are similar to those of Li^+ (Figure 11a), which is not surprising taking into account the metals' similar reduction potentials. For the Mn^{3+}/Mn^{4+} couple, the predicted voltages are 3.8 V (marokite) and 3.1 V (postspinel and spinel),[57,134] and for the Co^{3+}/Co^{4+} couple, the predicted voltages are 3.3 V ($Ca_3Co_2O_6$), 3.2 V ($Ca_3Co_4O_9$), and 3.8 V ($Ca_2Co_2O_5$).[185] As expected, the effect of the anion is critical to tune the intercalation potential, following the trends widely reported for Li materials.[136,181,186] Covalent hosts display lower voltages than the more ionic oxides, as evidenced by the predictions for the series of Chevrel phases: Mo_6S_8 (2.1 V), Mo_6Se_8 (2 eV), and Mo_6Te_8 (1.4 V).[131] A nice comparison is offered for oxo- vs thio-spinels,[57,121] where the calculated voltages for the Mn^{3+}/Mn^{4+} couple are 3 V for $CaMn_2O_4$ and 1.3 V for $CaMn_2S_4$. Similarly, the inductive effect raises the intercalation voltage in poly-oxoanionic compounds: the Mn^{2+}/Mn^{4+} couple is at 3.6 V for pyroxene-$CaMn(SiO_3)_2$ and 3.8 V for kutnahorite-$CaMn(CO_3)_2$.[154] Unfortunately, any comparison of these DFT predictions with experimental data is biased by issues related to the experimental setups (section 3); yet, some reported values are 3.5 V for $Ca_3Co_2O_6$[187] (DFT: 3.36 V[185]), 3.03 V for V_2O_5[35] (DFT: 3.28 V[120]), 1.5 V for TiS_2[124] (DFT: 1.7 V[183]), and no more than 1.3 V for MoO_3[188] (DFT: 2.23 V[188]). The large discrepancy for the latter supports that side-reactions might be taking place, as discussed in more detail in section 3.

Overall hosts with intercalation voltages of 2−3 V are appealing for electrolytes with low to medium anodic stability. Yet, given that electrolytes with higher anodic stabilities are developed,[78,79] the use of high-voltage cathodes (and here many oxides and poly-oxoanionic materials are in the 3−4 V range) would enable high-energy density Ca battery cells, pending the capacities.

The specific capacity for any intercalation host is dictated by the amount of Ca^{2+} that can be cycled between the oxidized and reduced state and the overall formula weight, and the former depends on the available crystallographic sites for Ca ions and the operating redox couples. If one considers for instance the perovskite structure $CaMO_3$, a frequent structural type for Ca−transition-metal oxides, looking at the crystallographic sites, the maximum theoretical capacity corresponds to the exchange of 1 Ca ion per TM, but this would drive the TM to have a formal oxidation state of +6, which is clearly unrealistic for most cases (excepted Mo).[132] Hence, theoretical capacities should be calculated considering reasonable TM oxidation states. The calcium cobalt oxides, $Ca_3Co_2O_6$, $Ca_2Co_2O_5$, and $Ca_3Co_4O_9$, is another set with the capacity being regulated by the redox couple (Co^{4+}/Co^{3+}), despite a larger amount of available Ca sites.[185] It is thus most often the oxidation states of the TM ions and not the available crystallographic sites which determine the maximum specific capacity for Ca cathodes. In such cases, the specific capacity is similar to that achievable by Li^+ intercalation. For TiS_2, DFT calculations predict a large voltage step at the stable intermediate $Ca_{0.5}TiS_2$ composition (Figure 11c),[128] with calculated average voltages of 1.7 V (Ti^{4+}/Ti^{3+}) and 0.9 V (Ti^{3+}/Ti^{2+}).[183] Hence, there would be a significant voltage drop if both redox couples were considered, and Ca insertion is likely limited to 0.5 mol Ca/TM and the Ti^{4+}/Ti^{3+} redox couple, delivering a similar specific capacity as 1 mol Li/TM. The consequence is that statements found claiming double specific capacity for Ca materials as compared to their Li analogues should be assessed carefully. Light TMs able to exchange two or more electrons are a priori: V^{3+}/V^{5+}, Mn^{2+}/Mn^{4+}, Cr^{3+}/Cr^{6+}, and Mo^{3+}/Mo^{6+} (not so light), and thus, their compounds should be the best candidates to surpass the capacities today achieved for Li cathodes.

For decades, the dream of the LIB research community has been to exchange two electrons per TM ion. As exposed by Goodenough, two redox couples can be accessed where the cation redox couples are "pinned" at the top of the O 2p bands, but to take advantage of this possibility, it must be realized in a framework structure that can accept more than one Li atom per transition-metal cation.[115,180] The latter requirement restricts the candidate materials, and in the Li-ion battery technology prompted attention to the Li_2MSiO_4 silicates (M= Fe, Mn, Co in tetrahedral sites) which could in theory exchange two electrons for each TM involving the M^{3+}/M^{2+} and M^{4+}/M^{3+} couples.[189−191] For these cathodes, the structural collapse driven by the instability of the tetrahedral TM ion as its oxidation state varies is a pending issue.[190,192] For Ca, this obstacle seems solvable as Ca^{2+} combines with octahedral Fe^{2+} and Mn^{2+} in major classes of minerals (pyroxene, garnets, double carbonates) and certain ternary oxides. Another great challenge in the LIB community is the effective utilization of the V^{5+}/V^{4+}, V^{4+}/V^{3+}, and even V^{3+}/V^{2+} redox couples,[117] and this also

DOI: 10.1021/acs.chemrev.9b00339
Chem. Rev. 2020, 120, 6331−6357

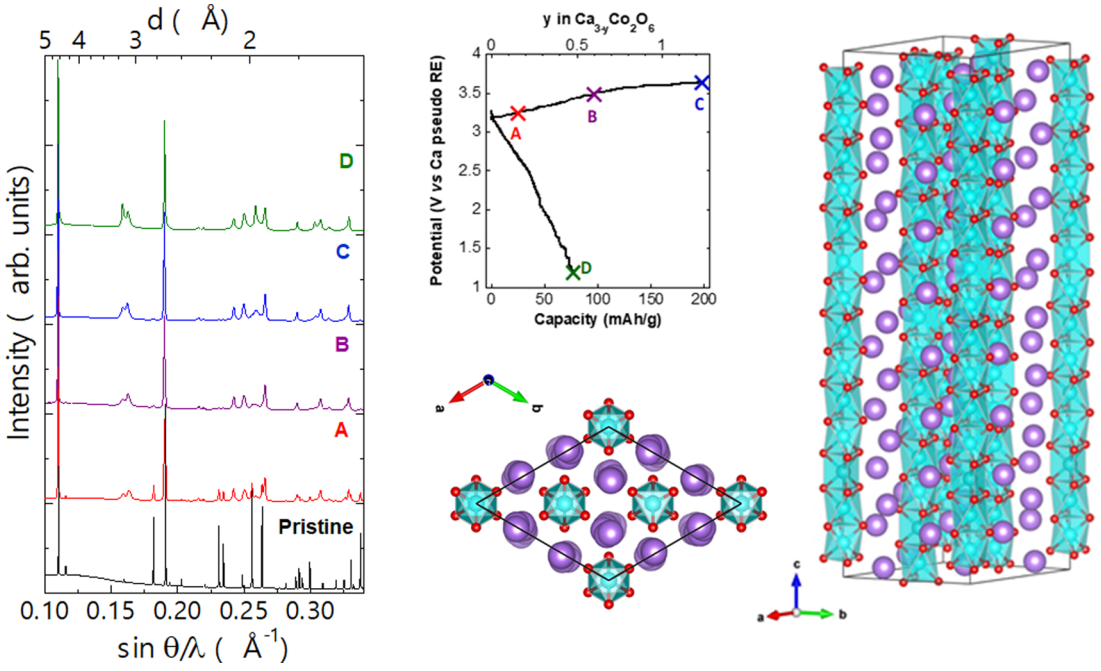

Figure 12. Potential vs capacity profiles from potentiodynamic cycling with galvanostatic acceleration (PCGA) experiments at 100 °C and C/200 rate in $Ca_3Co_2O_6$//Ca cells, progressively oxidized (labeled A in red, B in purple, C in blue) or oxidized and reduced (D in green), and corresponding diffraction patterns (black corresponding to pristine $Ca_3Co_2O_6$ electrode). The crystal structure of the oxidized $Ca_{2.3}Co_2O_6$ phase (corresponding to sample C) showing an incommensurate modulation is also depicted. Adapted from ref 187, copyright [2018] The Royal Society of Chemistry.

represents a priority route to achieve high-capacity Ca intercalation.

Realization of theoretical into practical capacities requires that the crystal and electronic structures are stable within the compositional limits of the intercalation reaction. Severe structural rearrangements are a major concern, and in the limit, irreversible structural phase transformations are a threat for reversible specific capacity even if they occur at the microstructure level.[193] Unit cell volume variation upon calcium deinsertion/insertion is a first measure and can be inferred from preliminary characterization: 18% for Ca_xTiS_2,[124] 1% for Ca_xMoO_3,[188] 3% for $Ca_xV_2O_5$,[43] and 3% for $Ca_xNaFePO_4F$.[194] Small volume variations found experimentally might, however, also indicate limited Ca insertion or even proton insertion. The actual amount of intercalation is often unknown, as side-reactions related to electrolyte decomposition might significantly contribute to the observed specific capacity, especially for tests carried out at high temperature, leading to overestimation in the value of x. For TiS_2 the measured specific capacity is 500 mAh/g, corresponding to an $x \approx 0.9$ nominal, while phases with $x \approx 0.2$ and 0.5 are detected by differential absorption tomography at the Ca L2 edge and XRD, respectively.[124]

Since the TM oxidation state varies along the charge/discharge of the battery, the host compound can become metastable with respect to other crystal structures at intermediate calcium contents. This is the case of Ca deinsertion from $Ca_3Co_2O_6$, for which DFT predicts a cell volume variation of 3% for 1 mol Ca extraction, which is in good agreement with experiments.[154,187] Regardless of the small volume variation, a phase transformation occurs upon Ca deinsertion. $Ca_3Co_2O_6$ crystallizes in the K_4CdCl_6-type structure[195] where the Co−O atoms form chains of alternating face-sharing CoO_6 octahedra and CoO_6 trigonal prisms along the hexagonal c-axis (Figure 12), separated by eight coordinated calcium atoms that according with DFT results[185] can diffuse in the structure albeit with sluggish kinetics. It has been demonstrated[187] that ca. 0.7 Ca ions can be extracted from $Ca_3Co_2O_6$ at ca. 3.5 V (Figure 12) but with a hindered reinsertion process presumably due to a large Ca desolvation energy at the electrolyte/electrode interface—hence, not an intrinsic property of the cathode material itself. The authors also concluded that Ca extraction results in the formation of a modulated structure with all Co ions in octahedral coordination,[196] and parallel DFT investigations[185] confirmed that the driving force for this phase transformation is the trend of Co ions to adopt octahedral coordination according with crystal field stabilization energies. In addition to this change, DFT indicates that the Ca sublattice rearranges making it unlikely to insert Ca ions to regain the initial $Ca_3Co_2O_6$. Under this perspective, irreveribility is an intrinsic issue of the material itself. Thus, further investigations with improved electrolyte formulations are needed to properly assess the reversible Ca intercalation in $Ca_2Co_2O_6$.

2.3.3. Diffusion in Host Materials. While the above-discussed capacity and voltage values determine the specific energy achievable, basically by thermodynamics, cathodes must also enable acceptable diffusion rates (kinetics) for the intercalated Ca^{2+} ions at any degree of insertion. Note that diffusivity may vary substantially with the host composition due to Coulombic repulsion between the diffusing Ca^{2+} ions and the TM cations in different oxidation states.[149,197] At present, limited mobility of the Ca^{2+} ions is one of the major concerns in multivalent cathode design. Factors determining diffusion are rooted in crystal chemistry; the pathways should be wide enough for the ions and exhibit a favorable topology to diminish the electrostatic interactions between the diffusing Ca^{2+} cation and the lattice constituents.

A good ionic diffusion coefficient ($D \approx 10^{-12}$ cm^2 s^{-1} for a C/2 rate) is a prerequisite for battery electrode materials. There are no direct measurements of Ca diffusion coefficients reported, and estimates from electrochemistry are hampered by the poor

DOI: 10.1021/acs.chemrev.9b00339
Chem. Rev. 2020, 120, 6331−6357

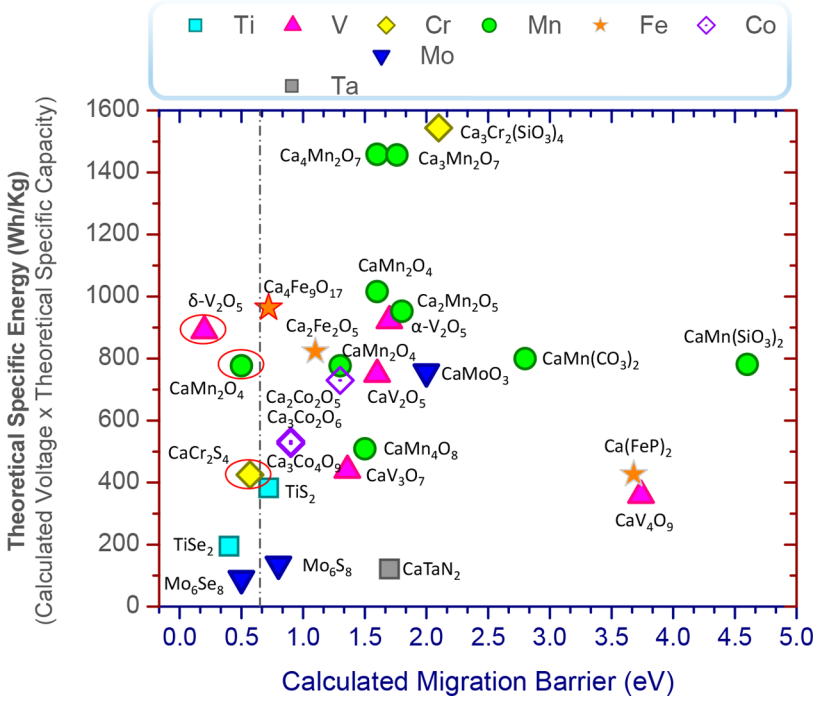

Figure 13. Theoretical specific energy vs calculated energy barriers (eV) for proposed Ca hosting TM compounds. The specific energy is estimated from the calculated average voltage for a particular redox couple and the corresponding theoretical specific capacity. The vertical line denotes the criterion for good cathode performance (<0.650 eV, see text). The red circles indicate virtual compounds. Data taken from 57, 120, 121, 131−134, 154, 182−185, 200, 201.

reliability of testing protocols and problems with the stabilities of electrolytes and interfaces (section 3). The migration energy barrier, i.e., the activation energy for an ionic hop, can be used as proxy,[149] and for a reasonable C-rate such as C/2, it should be <0.525 and <0.650 eV for micrometric and nanosized particles, respectively.[9,56] These barriers can be extracted from DFT calculations using the nudged elastic band method (NEB),[198] as shown in Figure 11b for a single A ion diffusing in a V_2O_5 lattice; the energy landscape along the diffusion path has a maximum at the saddle point, in this case, a face of the shared triangular face.

In Figure 13, reported calculated energy barriers for Ca migration in various TM compounds are depicted, and notably, <0.650 eV has been predicted for some virtual spinel-$Ca_T[M_2]_OO_4$ with Ca occupying the tetrahedral sites.[57] Rong et al. provided useful design guidelines to enhance ionic mobility in multivalent cathodes and identified the local topology and site preference as key parameters.[56] Hence, a good mobility was predicted in spinel-$Ca_T[M_2]_OO_4$, since the Ca ion would diffuse from a nonpreferred site (tetrahedral) to a preferred site (octahedral). Similarly, a barrier as low as 0.2 eV is predicted for the virtual δ-CaV_2O_5, where Ca ions occupy a nonpreferred site (bicapped-tetrahedral).[120] However, while such a δ-AV_2O_5 structure is known for A = Mg and Li, in the stable form of CaV_2O_5, the Ca ions adopt an 8-fold coordination.[199] Interestingly, the calculated barriers for the latter are >1.5 eV, in agreement with the unsuccessful attempts to extract Ca ions from CaV_2O_5.[125] Combining the above trends leads to the conclusion that metastable (and in many cases virtual) compounds are a better research target for unravelling calcium conducting cathodes. Yet, the already mentioned difficulties in synthesis, possible instability with cycling, and in general a voltage penalty are downsides of metastable materials.

In contrast, minerals are stable naturally occurring compounds. The garnet, pyroxene, and dolomite mineral groups all possess suitable Ca migration pathways, and promising capacities and voltages have been predicted for garnet-$Ca_3Cr_3Si_3O_{12}$ (uvarovite), pyroxene-$CaMn(SiO_3)_2$, and double carbonates-$CaMn(CO_3)_2$ (kutnahorite).[154] Nevertheless, their calculated energy barriers are larger than for oxides (Figure 13), with a maximum of 4 eV for the pyroxene. A possible reason for this is the higher concentration of cations in these 3D polyoxoanionic structures, arising from the transition metals and the silicate/carbonate groups. Paradoxically, the garnet structure is well-known for fast Li-ion conductors.[202,203] The hampered Ca mobility excludes not only these minerals but also the synthetic materials that exhibit these crystal structures. On the other hand, Lipson et al.[194] reported Ca intercalation into the layered structure of $NaFePO_4F$, boosting expectations of Ca intercalation in related 2D hosts.

The energy barriers >1.5 eV reported for perovskite-$CaMoO_3$, α-V_2O_5, and marokite-$CaMn_2O_4$ TM oxides (Figure 13) are in agreement with these materials being electrochemically inactive in Ca cells.[125,132134] In these oxides, the divalent charge of Ca^{2+} combines with its size to produce these large energy barriers. As a comparison, across ions, the migration barriers in α-$A_xV_2O_5$ (Figure 11b) follow the order $Li^+ < Mg^{2+} < Na^+ < K^+ < Ca^{2+} < Sr^{2+}$.[123] The same trend is reported for the marokite-$A_xMn_2O_4$, reaching a value of 1.8 eV for Ca^{2+}.[122,134] In both V_2O_5 and marokite, the diffusing A ions occupy eight-coordinated sites, which share a triangular face to form a channel running along one crystallographic direction. Triangular faces of the high-coordination-number polyhedra in V_2O_5 and marokite are too small to enable large cations through. This plays against Ca^{2+} diffusing better than Mg^{2+} ions in many inorganic structures. The larger rectangular faces shared by trigonal prisms seem more favorable for conduction of large cations (Ca^{2+}, Na^+, K^+), as inferred from the experimental diffusion coefficients for trigonal prismatically vs. octahedrally coordinated Na ions.[36,178]

DOI: 10.1021/acs.chemrev.9b00339
Chem. Rev. 2020, 120, 6331−6357

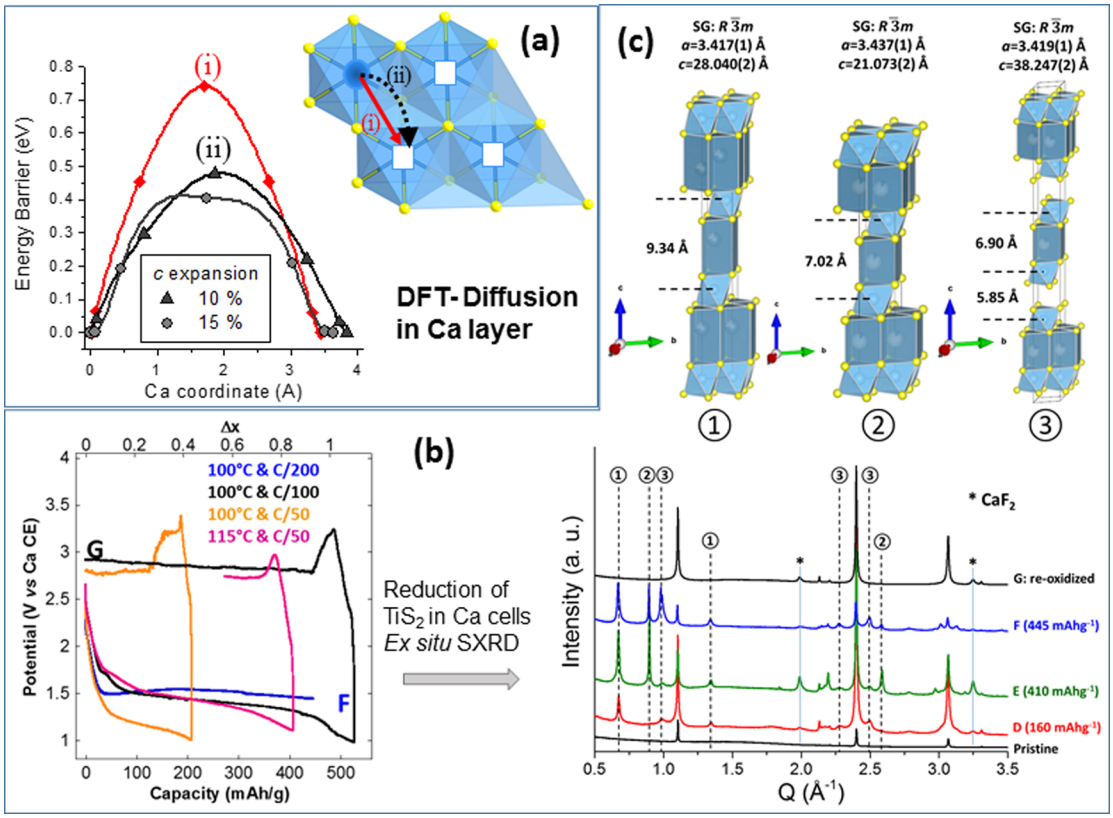

Figure 14. (a) Calculated energy barrier for Ca diffusion in TiS_2. The diffusing Ca ion jump from an occupied to a vacant octahedral site across either the S−S dumbbell (i) or the intermediate tetrahedral site (ii). (b) Curves from Ca//TiS_2 cells cycled at 100 °C and C/200 (blue), C/100 (black), and C/50 (orange) or at 115 °C and C/50 (pink). Note that the indicated potential is $E_{WE}-E_{CE}$. (c) SXRD collected at different stages of TiS_2 reduction in Ca cells and the associated refined structural model. For clarity, each pattern has been labeled with the corresponding capacity achieved upon reduction. Reprinted with permission from ref 124, copyright [2018] American Chemical Society.

Compared to monovalent cations, multivalent intercalants will suffer stronger electrostatic interactions with the surrounding cations (repulsive) and anions (attractive).[56,197] In the perovskite structure $CaMO_3$ (M = Cr, Mo, Mn, Fe, Co, Ni), the high energy barrier for Ca migration (2 eV) arises from the face-sharing between the transition-metal (TM) octahedra and the empty sites available for Ca diffusion.[132] In the related brownmillerite structure, which has a crystal structure analogous to the perovskite but with ordered oxygen vacancies, the latter defines a possible pathway for Ca diffusion, and weaker electrostatic repulsion lowers the calculated energy barrier down to 1.3 eV for $Ca_2Co_2O_5$[185] and 1.0 eV for $Ca_2Fe_2O_5$,[184] but this is still not low enough to consider them as viable Ca cathodes.

Chalcogenide networks provide better screening of electrostatic interactions and consequently lower the migration barriers—those calculated for Mo_6S_8 (0.8 eV),[182] Mo_6Se_8 (0.5 eV),[182] TiS_2 (0.72 eV),[124] and $TiSe_2$ (0.4 eV)[200] are so far the lowest reported for existing compounds. For reversible electrochemical Ca^{2+} intercalation in TiS_2 (Figure 14),[124] the first phase formed upon reduction is found to be the result of an ion-solvated intercalation mechanism, with solvent molecule(s) being cointercalated with the Ca^{2+} cation. Upon further reduction, new non-cointercalated calcium containing phases seem to form to the expense of unreacted TiS_2. In the noncointercalated phases, the Ca ions are likely in trigonal prismatic sites, in agreement with the above-discussed P3-structure stabilization for large intercalants[128] and forestalling an enhanced ionic mobility respective to the initial octahedral coordination. From the combination of experimental and computational techniques, it was concluded that the cation-solvated intercalation mechanism improves Ca^{2+} diffusion, by both expanding the interlayer space (here the DFT barrier lowers to 0.5 eV with a more stable transition state denoted as (ii) in Figure 14a) and the solvent-screened cation charge. In practice, however, solvent cointercalation should be avoided to enable high cell energy densities.

2.3.4. Alternative Cathode Materials. The overall sluggish Ca diffusion in inorganic intercalation host materials is a major concern for enabling useful high-energy rechargeable Ca batteries with reasonable power performance. Alternative cathode concepts are therefore given attention, including organic electrodes offering mechanical flexibility, mild synthesis approaches, processability, and ample structural and chemical tuneability that can result in high specific capacities, up to 500 mAh/g for quinones, at attractive intercalation voltages.[204−206] A circular battery economy is viable by preparing the materials from renewable sources.[207,208] The limitations are primarily the large solubility of active material in electrolytes, capacity fading, and low rate performance. Even if many advances have been made within different classes of organic cathodes: carboxylates, organic radicals, quinones, imides, and so on, for Li and Na batteries,[204−206,209] investigations in organic electrodes for Ca batteries are so far limited to anodes in aqueous batteries, as previously discussed in section 2.1.2.[96,97]

Also, sulfur and air cathodes have been suggested for Ca batteries—thus, Ca/S and Ca/air batteries, respectively.[20,45,103,210] While such cathodes and battery concepts

DOI: 10.1021/acs.chemrev.9b00339
Chem. Rev. 2020, 120, 6331−6357

Table 2. Summary of Electrochemical Test for Ca Cathodes in Either Three- or Two-Electrode Cell Configuration

positive electrode	negative electrode	reference electrode	electrolyte	V range	capacity (mAh/g)	cycles	comments
V_2O_5[35,44]	activated carbon	Ag	0.5 M $Ca(ClO_4)_2$ in PC	1 to −0.5	200/465	3/8	(xerogel/PC composite VOx/PC)
V_2O_5[42,43]	Ca	$Ag/AgNO_3$	1 M $Ca(ClO_4)$ in ACN	−0.5 to −1.5	400	0.5	XRD of "intercalated phase" given.
V_2O_5[125]	Ca	Ca	0.3 M $Ca(ClO_4)_2$ in ACN 0.3 M $Ca(BF4)_2$ in EC:PC 0.3 M $Ca(TFSI)_2$ in EC:PC 0.3 M $Ca(ClO_4)_2$ in EC:PC (100 °C)	0 to 3	200−600	0.5	Capacity attributed to side-reactions involving the electrolyte.
V_2O_5[170]	activated carbon	Ag	0.5 M $Ca(TFSI)_2$ in EC:PC water content from H_2O/Ca = 0 to 9.5	1 to −1.5	150	5	Water has an influence in overpotential. XRD given.
CaV_2O_5[125]	Ca	Ca	0.45 M $Ca(BF_4)_2$ in EC:PC (100 °C)	3.6 to 2.6	250	0.5	Capacity attributed to side-reactions involving the electrolyte, enhanced at high T. Attempts of chemical oxidation using NO_2BF_4 also unsuccessful.
$NH_4V_4O_{10}$[227]	Pt	$Ag/AgNO_3$	1 M $Ca(ClO_4)_2 \times H_2O$ in ACN	1 to −0.2	100	100	Changes in XRD reported, but mechanism not fully elucidated.
$Ca_{0.5}Co_2O_4$[164]	V_2O_5	-	0.5 M $Ca(ClO_4)_2$ in ACN	1 to 0	80	30	XPS/XRD to study mechanism but not fully elucidated.
$Ca_3Co_2O_6$[187]	Ca	Ca	0.45 M $Ca(BF_4)_2$ in EC:PC 100 °C	3.5 to 1	150	0.5	Reversibility very limited, if any.
MoO_3[188]	Ca	Ca	0.5 M $Ca(TFSI)_2$ in DME	2.2 to 0.7	80	12	XPS/XRD/Raman XRD similar to protonated phase.
MoO_3[188]	activated carbon	-	0.1 M $Ca(TFSI)_2$ in ACN	2.8 to 0.8	150	5	
MoO_3[228]	activated carbon	$Ag/AgNO_3$	0.5 M $Ca(TFSI)_2$ /AN	1 to −1	120	3	XPS and XRD, but mechanism not elucidated.
$K_{0.31}MnO_2 \cdot 0.25H_2O$ (birnessite)[229]	activated carbon	Ag/AgCl	1 M $Ca(NO_3)_2$ $4H_2O$ in water	0.9 to −0.4	150	50	XRD, EDX, possibly proton participation.
$Mg_{0.19}Na_{0.07}MnO_2 \cdot 0.37H_2O$ (todorokite)[230]	Ca and V_2O5 (two counterel)	$Ag/AgNO_3$	0.2 M $Ca(CF_3SO_3)_2$ in ACN	1 to −2	100	10	XAS, but mechanism not fully elucidated.
$K_2BaFe(CN)_6$[231]	carbon paper	Ag/AgCl	1 M $Ca(ClO_4)_2$ in ACN	0 to 0.8	55.8	100	
$Na_{0.2}MnFe(CN)_6$[100]	Ca_xSn	Ca^{2+}/Ca	0.2 M $Ca(PF)_6$ in EC + PC	0 to 3.5	70	35	
$KNiFe(CN)_6$[54]	activated carbon	Ag^+/Ag	0.5 M $Ca(TFSI)_2$ in ACN	−1 to 1	60	12	
TiS_2[124]	Ca	Ca	0.45 M $Ca(BF_4)$ in EC:PC 100 °C	3.5 to 1	48	2	Electrolyte solvent cointercalation, Ca insertion assessed by tomography.
TiS_2[45]	Li	-	0.1 M $Ca(CF_3SO_3)_2$ in PC or PC:DMC	3 to 1.5	100	3	Minor changes in XRD, Li present as Li counter electrode.
Mo_6Se_8[232]	$CaHg_{11}$−Ca	$CaHg_{11}$−Ca	0.5 M $Ca(ClO_4)_2$ in ACN 25−75 °C	2 to 0.4	3−10	100	
$NaFePO_4F$[194]	carbon	-	0.2 M $Ca(PF_6)_2$ in EC:PC 3:7	−1.5 to 3	80	50	Changes in XRD reported, but mechanism not fully elucidated.
$CaTaN_2$[201]	Ca	Ca	0.45 M $Ca(BF_4)_2$ in EC:PC (100 °C)	4.5 to 0.5	60	1	Loss of crystallinity upon oxidation.
graphite[82]	Sn	-	0.8 M $Ca(PF_6)_2$ in EC:PC:DMC:EMC (2:2:3:3)	3 to 5	70	350	Graphite cathode operating through a redox mechanism based on anion intercalation. XRD consistent with the presence of very crystalline Ca_7Sn_6 after 300 cycles.
S infiltrated mesoporous carbon[45]	Ca	$Ag/AgClO_4$	0.5 M $Ca(ClO_4)_2$ in ACN	0.75	600	0.5	Primary system. Nature of reduction products not fully elucidated.
O_2[64]		Ag^+/Ag	0.4 M $Ca(ClO_4)_2$ in DMSO				Superoxide and peroxide detected upon reduction by differential electrochemical mass spectroscopy.

DOI: 10.1021/acs.chemrev.9b00339
Chem. Rev. 2020, 120, 6331−6357

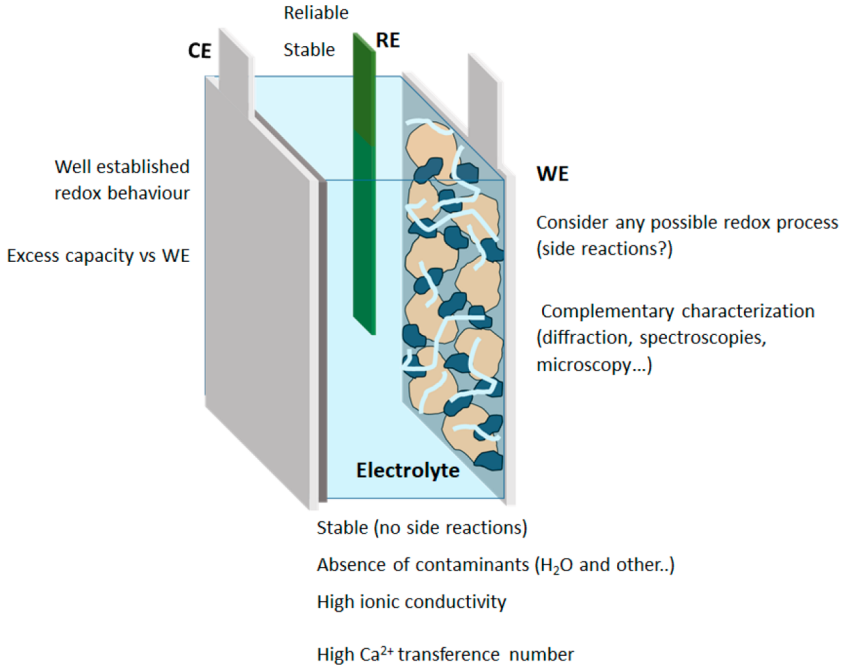

Figure 15. Scheme of a three-electrode Ca metal-anode-based cell setup with key properties to be developed/studied.

hold promise of very low cost and potentially would be an option for large scale energy storage, significant bottlenecks remain to be addressed—many of them covered in the research on Li/S and Li/air batteries.[211] We note the "early" work on Ca/S resulting in rather high-capacity cells, but primary batteries due to an irreversible process upon reduction are still not well-understood.,[45] Nevertheless, the large potential, primarily in terms of cost and energy density, calls for further investigations.[210] The Ca/air concept is truly challenging and besides early papers discussing the possibility of operating a cell at high temperature,[20] there has been limited research efforts to develop systems operating at room temperature using a DMSO-based electrolyte suggested to allow formation of a Ca superoxide.[64] Some insoluble side-products were obtained but were not fully characterized, while the soluble species seem to reoxidize to oxygen with high Coulombic efficiency despite a high overpotential and with a reversibility decreasing as a function of water content in the electrolyte.[64] So far, no studies have been reported dealing with operation of an oxygen electrode using electrolytes enabling reversible calcium plating and stripping, despite that some efforts have been reported using ionic-liquid-based electrolytes.[63] Overall it is clear that there is a long way to go before any reliable proof-of-concept can be achieved and the true technological prospects are evaluated.[103]

3. EXPERIMENTAL SETUPS, METHODOLOGY DEVELOPMENT, AND FULL-CELL ASSESSMENTS

While the previous sections have approached the Ca battery from a materials perspective, and in many cases, predicted and theoretical performance is quoted, Table 2 summarizes the practical achievements to date for different materials and a wide range of setups. However, before discussing the results in detail, the experimental protocols are to be covered as developing new battery chemistries is far from being trivial and the absence of any reliable standards makes the process tricky. Figure 15 highlights various complexities in the experimental setup of Ca cell studies and construction.

Starting with electrochemical setups, for technologies such as LIBs, new electrode materials are simply tested using a standard electrolyte and vice versa, typically in two-electrode cells with lithium metal as both the counter and reference electrode (a so-called half-cell). For less well-studied systems, the use of a separate reference electrode (through which no current flows) in a three-electrode cell setup is compulsory to be able to independently control and monitor the behavior of the working/counter electrode within the cell and assist in ascertaining the origin of observed features. The choice of the reference electrode is, however, not trivial.[101] Silver wires have been often used as pseudo-reference electrodes when testing new cathode materials, but their potential is highly dependent on the anion present in the electrolyte. To address this issue, strategies such as calibration with a well-known standard as Fc^+/Fc or use of a reference electrode cell compartment in which the wire is in contact with a specific electrolyte have been used.[212] While calcium metal would be the first obvious choice as a counter electrode for cathode development, the fact that plating/stripping is only viable under very specific conditions casts severe restrictions on its domain of application. If used in electrolytes not enabling calcium plating, reduction of the working electrode would be feasible (if calcium stripping takes place at the counter electrode), but reoxidation of the working electrode would result in unknown redox processes at the counter electrode, most likely related to electrolyte decomposition, which may affect the electrolyte speciation and the electrochemical response. Instead, activated carbon has often been used (Tables 1 and 2), operating through a capacitive mechanism, but electrode balancing is not trivial and rarely mentioned. Oversizing the capacitive counter electrode, which typically has low capacity, vs the electrode material to be investigated, most often operating through a faradaic redox mechanism and, hence, higher capacity, can be cumbersome in a practical cell. Despite a Sn−Ca alloy being reported as a counter electrode for testing $Na_{0.2}MnFe(CN)_6$, its capacity was very low, <50 mAh/g, and the electrochemical alloying not fully assessed,

DOI: 10.1021/acs.chemrev.9b00339
Chem. Rev. 2020, 120, 6331−6357

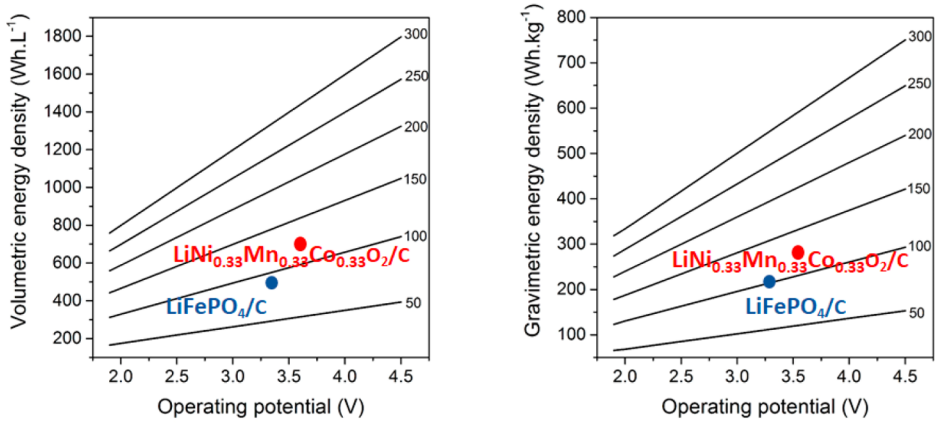

Figure 16. Volumetric and gravimetric energy densities for hypothetical calcium metal-based batteries. The straight lines are calculated energy densities as a function of operation potential and capacities (denoted on the right of each line) of the positive electrode material. All calculations were made using the model developed by Berg et al.[226] Reproduced with permission from ref 225. Copyright 2019 Frontiers.

the electrolyte side-reactions were inferred.[100] Formation of crystalline Ca_7Sn_6 after 300 cycles when using Sn foils as anodes has been reported[82] but also with electrolyte decomposition products being detected on the electrode surface.

Another factor affecting the electrochemical setup and results is that very few calcium salts are commercially available, and the most commonly used salt is $Ca(ClO_4)_2$. This salt is typically hydrated and also difficult to obtain in anhydrous form due to its explosive nature. This means that many results in the literature are likely obtained in the presence of a non-negligible amount of water in the electrolyte, seldom reported in the experimental sections until very recently, which may result in side-reactions such as H^+/H_3O^+ intercalation or water reduction/oxidation. This in turn can result in some observed "false" electrochemical capacity, as was reported for Mg^{2+} intercalation in V_2O_5.[102] While the $Ca(TFSI)_2$ and $Ca(CF_3SO_3)_2$ salts also are commercial but much less used, the synthesis of $Ca(PF_6)_2$ was reported only very recently[83,100] but with purity issues due to a very high tendency of anion hydrolysis. $Ca(NO_3)_2$ is the salt most commonly used in aqueous electrolytes, and again, side-reactions related to H^+/H_3O^+ intercalation probably deserve further investigation, as these have been shown to be an issue for Zn^{2+}-based aqueous chemistries,[213] and there are no major reasons to believe that the situation would be different for Ca^{2+}.

Moving from pure electrochemical setups, the use of advanced materials characterization techniques is often warranted to properly assess and understand the Ca intercalation reactions, in particular to elucidate the real intercalation degree and associated structural changes in cathodes as well the nature and composition of the interfaces created between anodes and electrolytes.

To properly consider the length scale that can be probed, e.g., surface for XPS, bulk for XRD, and atomic for TEM (transmission electron microscopy), is also a must.[214−218] Moreover, the precision and reliability of each technique also deserves attention as well as if ex situ, in situ, and/or operando setups are to be preferred. For instance, the amount of intercalated Ca ions cannot be assessed from the electrochemical capacity unless the absence of side-reactions can be confirmed, including issues such as simple corrosion of current collectors.[219] Chemical analysis techniques such as inductively coupled plasma (ICP), atomic absorption (AAS), and energy dispersive (EDS) spectroscopy can possibly be applied, but these methods may all overestimate the degree of Ca^{2+} insertion, as there might be calcium containing electrolyte salt residues or surface layers resilient to the sample preparation of washing, as shown for Mg^{2+} intercalation studies.[220] In the absence of reliable structural determination of the phases involved in the redox mechanism showing crystal sites and occupation for calcium ions or in the presence of mixed and/or amorphous phases, spectroscopic techniques specifically probing calcium are useful.[221] This is especially true if a 3D distribution can be achieved by tomography—a technique which recently enabled to unambiguously detect reversible calcium intercalation in TiS_2.[124]

Also, the polymorphs used can be an issue and not always under control. V_2O_5 has attracted a lot of attention for Ca batteries and despite some studies dealing with samples prepared in the laboratory, including a xerogel composite (Table 2), most studies deal with the commercially available orthorhombic α-V_2O_5, for which a slight increase of the *a* cell parameter was reported in the very first studies of calcium cells.[42,43] The redox process was then assumed to result in a significant amount of calcium intercalation, but no structural model was provided. The XRD diffraction pattern is, however, different from that of the isostructural α-CaV_2O_5 obtainable by solid-state synthesis[222,223] and also from the δ-polymorph, for which lower migration barrier was predicted[129,224] and which seems to be unstable with respect to the α-structure. Instead, there are notable similarities to the patterns observed for some $H_xV_2O_5$ and $H_xV_4O_{10}$ phases, a fact clearly deserving further attention.[125] Attempts to electrochemically oxidize α-CaV_2O_5 did not result in any change in the XRD pattern, in agreement with the high-energy migration barriers for Ca^{2+} predicted for this polymorph (discussed in section 2.3).[129,224] Combining all of the above makes us propose that the electrochemical capacity observed likely is related to electrolyte decomposition and possibly proton insertion, at least partially—further stressing the need for combined electrochemical and advanced material analysis.

In line with the above, the electrochemical reduction of MoO_3 in calcium containing electrolytes has been shown to result in changes in the Mo oxidation state, and XRD indicates the formation of a new phase for which the Ca content could not be fully assessed.[225] The authors comment that it exhibits the *Cmcm* space group, a space group previously reported for some H_xMoO_3 phases.[164,188]

DOI: 10.1021/acs.chemrev.9b00339
Chem. Rev. 2020, 120, 6331−6357

Prussian blue analogues (PBAs) present even more complexity, as these materials are known to exhibit variable amounts of water in their crystal structures. This water is sometimes difficult to remove, and also, the versatility of PBA structural frameworks results in difficulties to extract meaningful data of occupation sites and factors from XRD. Yet, given the good rate performance reported to date for intercalation of single-valent ions, especially using aqueous electrolytes,[213] further exploration of the mechanisms taking place in divalent systems should be encouraged.

Last but not least, care should be exercised in generalizing results achieved for a specific electrolyte. Besides the possibility of side-reactions occurring due to insufficient (electro-)chemical stability, there are many other intrinsic issues related to the electrolyte composition, e.g., viscosity—affecting both ion transport and wetting of the electrodes, ion−ion and ion−solvent interactions, (de)solvation dynamics, and so on, which also may affect the electrode behavior. Recent reports demonstrate that Ca ions can be extracted from $Ca_3Co_2O_6$[187] and $CaTaN_2$,[201] but the insertion processes are elusive. Here the lack of reversibility could be attributed either to, e.g., a difficult Ca desolvation during discharge or to intrinsic cathode material properties/decomposition reactions.

Despite the numerous challenges remaining with respect to the development of functional Ca cells, the promising results of some chemistries (TiS_2, $Ca_3Co_2O_6$) call for realistic estimates of (prospective) full-cell figures of merit. To quantify these at the cell level, the energy-cost model developed by Berg et al.[226] was used.[225] Using a scheme of possible operation potentials and specific capacities of some selected existing or virtual materials, the energy densities for a set of different cell configurations were estimated and benchmarked vs other rechargeable battery technologies, including LIBs (Figure 16). Specific LIB technologies are depicted with symbols, while the calcium concepts are represented by straight lines of energy densities as a function of operating voltage and specific capacity of the cathodes. The results indicate that the theoretical energy densities for calcium batteries could easily top the state-of-the-art LIBs while most likely being cheaper. Overall, even cells with only moderate operating voltages of 2.1 or 2.5 V and cathode capacities of 250 or 200 $mAh \cdot g^{-1}$ would yield higher energy densities than the best state-of-the-art LIBs. Moreover, for combinations of 3.0 V/250 $mAh \cdot g^{-1}$ or 3.5 V/200 $mAh \cdot g^{-1}$, the volumetric energy densities would be >1000 $Wh \cdot L^{-1}$, hence higher than any of the (prospective) sulfur-cathode-based battery technologies. The cost-effectiveness for the battery configurations was also estimated, indicating that calcium batteries would be on par with state-of-the art graphite/NMC LIBs even for very high hypothetical calcium cathode material costs (>80 $\$ \cdot kg^{-1}$).

4. CONCLUDING REMARKS

Reviewing the state-of-the-art of rechargeable Ca batteries, we find that most studies focus on developing inorganic intercalation host materials possessing TM ions combined with a variety of simple or complex anions (oxides, sulfides, hexacyanoferrates, etc.), electrolytes with high anodic stability able to reversibly plate/strip Ca metal efficiently, and the anode/electrolyte interface. Very few, if any, full-cell studies exist, which both assures that the reported capacities truly originate in the redox reactions aimed for and at the same time covers all the aspects we today take for granted for the LIB technology: capacity fading at different C-rates and associated Coulombic efficiencies, calendar/shelf life vs cycle-life assessments, and so on. Indeed, very few studies are able to even name a target application due to the incomplete characteristics at hand—which though is natural at this early stage of development. According to energy-cost models, however, the prospects for the Ca battery technology are encouraging, and this is further strengthened by the current technology advances—both on the materials and cell levels. Alternative directions such as Ca/O_2 and Ca/S batteries might be feasible, but must solve the same intrinsic bottlenecks associated with air and sulfur electrodes that are not yet mastered for the corresponding Li, Na, or Mg technologies and might in some aspects be even more difficult for Ca-based batteries, e.g., the very stable CaO potentially being formed.

The battery performance possible to attain certainly depends on the intrinsic material properties. Along this Review we have, however, underlined that the actual observation of electrochemical activity in laboratory cells requires using appropriate testing protocols and cell configurations—not the least when new chemistries are to be explored. The literature offers several examples of "failed" experiments dealing with materials not showing electrochemical activity. This may be due to a diversity of causes, such as bad inherent properties of the electrode materials, issues related to electrolyte degradation, or to difficult Ca desolvation at the interfaces, and therefore exemplifies the need for improved and a variety of experimental setups—not the least complementing the electrochemical by advanced materials analysis. As long as findings are rationalized and rigorously discussed, any result (positive or negative) represents a small step in the long and winding road to the design of new battery technologies, in general, and calcium-based systems, in particular. Finally, we would like to stress that since the current trend of the increasing need of batteries both in sheer amount but also in terms of diversification, devices, and applications, is expected to progress more rapidly in the not-so-distant future, the development of different and complementary battery technologies to the prevailing LIBs of today is the only long-term sustainable strategy. Herein, Ca batteries surely have a role to play.

AUTHOR INFORMATION

Corresponding Authors

*E-mail: e.arroyo@quim.ucm.es. (M.E.A.D.)
*E-mail: rosa.palacin@icmab.es. (M.R.P.)

ORCID

M. Elena Arroyo-de Dompablo: 0000-0001-5249-3562
Alexandre Ponrouch: 0000-0002-8232-6324
Patrik Johansson: 0000-0002-9907-117X
M. Rosa Palacín: 0000-0001-7351-2005

Notes

The authors declare no competing financial interest.

Biographies

M. E. Arroyo-de Dompablo is Professor in Inorganic Chemistry at Universidad Complutense de Madrid (UCM), Spain. She received her Ph.D. degree in Chemistry from UCM in 1998 and was appointed postdoctoral associate in the Department of Materials Science and Engineering at Massachusetts Institute of Technology from 2000 to 2003, to undertake computational investigations in materials for energy storage. Her research interest focuses on the combination of experimental and computational techniques to investigate various

DOI: 10.1021/acs.chemrev.9b00339
Chem. Rev. 2020, 120, 6331−6357

areas of solid-state chemistry, including materials for rechargeable batteries and transformations of solids under high-pressure conditions.

Alexandre Ponrouch is currently a staff researcher at the Institut de Ciència de Materials de Barcelona (ICMAB-CSIC). He received his Ph.D. from the Institut National de la Recherche Scientifique (INRS-EMT, Canada) in 2010 working on electrodeposition of metals, alloys, and oxides for application in fuel cells and supercapacitors. He further joined ICMAB-CSIC to embrace research in battery electrolytes. His current research is mainly focused on developing new electrolytes for multivalent batteries following fundamental electrochemistry approaches.

Patrik Johansson is Full Professor in Physics at Chalmers University of Technology, Gothenburg, Sweden, which he joined in 1999. He has a Ph.D. in Inorganic Chemistry from Uppsala University, Sweden (1998), and he made a postdoctoral stay at Northwestern University. He is currently codirector of ALISTORE-ERI (CNRS FR 3104), Europe's largest industry−academia network within the field of modern batteries. His science combines understanding of new materials, mainly various electrolytes, at the molecular scale with next generation battery concept development and real battery performance—both via experimental and modeling efforts.

M. Rosa Palacín is a research Professor at the Institut de Ciència de Materials de Barcelona (ICMAB-CSIC) and actively involved in ALISTORE-ERI (which she codirected 2010−2017). After a Ph.D. in solid-state chemistry (UAB, 1995) and a postdoctoral stay at LRCS (Amiens, France), her research career at ICMAB-CSIC has been fully focused in rechargeable battery materials with specific emphasis set in the study of electrode materials. She worked on nickel-based and lithium-based technologies to more recently deviate to alternative chemistries such as sodium-ion and also multivalent systems.

ACKNOWLEDGMENTS

Funding from the European Union's Horizon 2020 research and innovation programme H2020 FETOPEN-1-2016-2017 (CARBAT, grant agreement No. 766617) and ERC-2016-STG, (CAMBAT grant agreement No 715087) is gratefully acknowledged. A.P., P.J., and M.R.P. are grateful for the stimulating discussions within the ALISTORE-ERI network. A.P. and M.R.P. are grateful to the Spanish Ministry for Economy, Industry and Competitiveness Severo Ochoa Programme for Centres of Excellence in R&D (SEV-2015-0496). M.E.A.D. thanks J. Carrasco for kindly sharing his results on V_2O_5 and the MALTA-Consolider network for computational resources (CSD2007-00045, MAT2015-71070-REDC). P.J. acknowledges the financial support from the Swedish Energy Agency (contract #37671-1, Next Generation Batteries) and Chalmers Battery Initiative, part of the profile Materials for Energy Applications jointly managed by the Areas of Advance Materials Science and Energy at the Chalmers University of Technology.

REFERENCES

(1) Nykvist, B.; Nilsson, M. Rapidly Falling Costs of Battery Packs for Electric Vehicles. *Nat. Clim. Change* **2015**, *5*, 329−332.
(2) Sarma, D. D.; Shukla, A. K. Building Better Batteries: A Travel Back in Time. *ACS Energy Lett.* **2018**, *3*, 2841−2845.
(3) Winter, M.; Barnett, B.; Xu, K. Before Li Ion Batteries. *Chem. Rev.* **2018**, *118*, 11433−11456.
(4) Ponrouch, A.; Palacín, M. R. Post-Li Batteries: Promises and Challenges. *Philos. Trans. R. Soc., A* **2019**, *377*, 20180297.
(5) Abraham, K. M. Directions in Secondary Lithium Battery Research-and-Development. *Electrochim. Acta* **1993**, *38*, 1233−1248.
(6) Scrosati, B. Lithium Rocking Chair Batteries - an Old Concept. *J. Electrochem. Soc.* **1992**, *139*, 2776−2781.
(7) Tarascon, J. M.; Guyomard, D. The $Li_{1+X}Mn_2O_4$/C Rocking-Chair System - a Review. *Electrochim. Acta* **1993**, *38*, 1221−1231.
(8) Muldoon, J.; Bucur, C. B.; Gregory, T. Quest for Nonaqueous Multivalent Secondary Batteries: Magnesium and Beyond. *Chem. Rev.* **2014**, *114*, 11683−11720.
(9) Canepa, P.; Sai Gautam, G.; Hannah, D. C.; Malik, R.; Liu, M.; Gallagher, K. G.; Persson, K. A.; Ceder, G. Odyssey of Multivalent Cathode Materials: Open Questions and Future Challenges. *Chem. Rev.* **2017**, *117*, 4287−4341.
(10) Haring, H. E.; Thomas, U. B. The Electrochemical Behavior of Lead, Lead-Antimony and Lead-Calcium Alloys in Storage Cells. *Trans. Electrochem. Soc.* **1935**, *68*, 293−307.
(11) Thomas, U. H.; Forster, F.; Haring, H. E. Corrosion and Growth of Lead-Calcium Alloy Storage Battery Grids as a Function of Calcium Content. *Trans. Electrochem. Soc.* **1947**, *92*, 313−325.
(12) Salkind, A. J.; Cannone, A. G.; Trumbure, F. A. Lead-Acid Batteries. In *Handbook of Batteries*, 3rd ed.; Linden, D., Reddy, T. B., Eds.; McGraw Hill: New York, 2002.
(13) Selis, S. M.; Wondowski, J. P.; Justus, R. F. A High-Rate, High-Energy Thermal Battery System. *J. Electrochem. Soc.* **1964**, *111*, 6−13.
(14) McManis, G. E.; Miles, M. H.; Fletcher, A. N. Performance and Discharge Characteristics of Ca/LiCl, $LiNO_3$/$LiNO_3$, $AgNO_3$/Ni Thermal Battery Cells. *J. Electrochem. Soc.* **1984**, *131*, 283−286.
(15) Clark, R. P.; Grothaus, K. R. An Improved Calcium Anode for Thermal Batteries. *J. Electrochem. Soc.* **1971**, *118*, 1680−1683.
(16) Nissen, D. A. Study of the Anode-Electrolyte Interface in a Thermal Battery. *J. Electrochem. Soc.* **1979**, *126*, 176−180.
(17) Miles, M. H.; Dine, D. A.; Fletcher, A. N. The Calcium Anode in Molten Nitrate Electrolytes. *J. Electrochem. Soc.* **1978**, *125*, 1209−1214.
(18) Schoonman, J.; Wolfert, A. Alloy-Anodes in Fluoride Solid-State Batteries. *J. Electrochem. Soc.* **1981**, *128*, 1522−1523.
(19) Sammells, A. F.; Schumacher, B. Secondary Calcium Solid Electrolyte High-Temperature Battery. *J. Electrochem. Soc.* **1986**, *133*, 235−236.
(20) Pujare, N. U.; Semkow, K. W.; Sammells, A. F. A Calcium Oxygen Secondary Battery. *J. Electrochem. Soc.* **1988**, *135*, 260−261.
(21) Staniewicz, R. J. A Study of the Calcium-Thionyl Chloride Electrochemical System. *J. Electrochem. Soc.* **1980**, *127*, 782−789.
(22) Peled, E.; Meitav, A.; Brand, M. Calcium Thionyl Chloride High-Rate Reserve Cell. *J. Electrochem. Soc.* **1981**, *128*, 1936−1938.
(23) Meitav, A.; Peled, E. Calcium-Ca$(AlCl_4)_2$-Thionyl Chloride Cell - Performance and Safety. *J. Electrochem. Soc.* **1982**, *129*, 451−457.
(24) Peled, E.; Tulman, R.; Golan, A.; Meitav, A. Calcium/Ca$(AlCl_4)_2$ - Thionyl Chloride High-Rate Cell. *J. Electrochem. Soc.* **1984**, *131*, 2314−2316.
(25) Meitav, A.; Peled, E. Solid Electrolyte Interphase (SEI) Electrode 0.5. The Formation and Properties of the Solid Electrolyte Interphase on Calcium in Thionyl Chloride Solutions. *Electrochim. Acta* **1988**, *33*, 1111−1121.
(26) Binder, M.; Gilman, S.; Wade, W. Calcium-Sulfuryl Chloride Primary-Cell. *J. Electrochem. Soc.* **1982**, *129*, 897−899.
(27) Peled, E.; Tulman, R.; Meitav, A. Solid Electrolyte Interphase (Sei) Electrodes 0.6. Calcium-Ca$(AlCl_4)_2$-Sulfuryl Chloride System. *J. Power Sources* **1983**, *10*, 125−135.
(28) Peled, E.; Elster, E.; Tulman, R.; Kimel, J. Calcium Ca$(AlCl_4)_2$-Thionyl Chloride (TC) Cell - Effect of Temperature and Cell Parameters on Performance. *J. Power Sources* **1985**, *14*, 93−98.
(29) Elster, E.; Cohen, R.; Peled, E. Solid Electrolyte Interphase (SEI) Electrodes 0.7. The Electrochemical-Behavior of Calcium in Ba$(AlCl_4)_2$ and Sr$(AlCl_4)_2$ Thionyl Chloride Solutions. *J. Power Sources* **1989**, *26*, 423−425.
(30) Peled, E.; Cohen, R.; Melman, A.; Lavi, Y. Calcium-$SOCl_2$ Cell - Effect of Can Material and Polarity on Storage Properties. *J. Electrochem. Soc.* **1992**, *139*, 1836−1839.
(31) Bradley, J.; Mitchell, P. Current Status of Calcium Thionyl Chloride Batteries. *Chem. Ind.* **1990**, *5*, 135−137.

DOI: 10.1021/acs.chemrev.9b00339
Chem. Rev. 2020, 120, 6331−6357

(32) Aurbach, D.; Skaletsky, R.; Gofer, Y. The Electrochemical-Behavior of Calcium Electrodes in a Few Organic Electrolytes. *J. Electrochem. Soc.* **1991**, *138*, 3536−3545.
(33) Blomgren, G. The Development and Future of Lithium Ion Batteries. *J. Electrochem. Soc.* **2017**, *164*, A5019−A5025.
(34) Aurbach, D.; Lu, Z.; Schechter, A.; Gofer, Y.; Gizbar, H.; Turgeman, R.; Cohen, Y.; Moshkovich, M.; Levi, E. Prototype Systems for Rechargeable Magnesium Batteries. *Nature* **2000**, *407*, 724−727.
(35) Amatucci, G. G.; Badway, F.; Singhal, A.; Beaudoin, B.; Skandan, G.; Bowmer, T.; Plitz, I.; Pereira, N.; Chapman, T.; Jaworski, R. Investigation of Yttrium and Polyvalent Ion Intercalation into Nanocrystalline Vanadium Oxide. *J. Electrochem. Soc.* **2001**, *148*, A940−A950.
(36) Whittingham, M. S. Chemistry of Intercalation Compounds - Metal Guests in Chalcogenide Hosts. *Prog. Solid State Chem.* **1978**, *12*, 41−99.
(37) Le Blanc-Soreau, A.; Rouxel, J. Facteurs Physiques Et Structuraux Dans Les Systèmes D'intercalaires: Systèmes $A_x^{+2}TiS_2$, Cas Du Calcium. *C. R. Seances Acad. Sci., Ser. C* **1974**, *279*, 303−306.
(38) Lerf, A.; Schollhorn, R. Solvation Reactions of Layered Ternary Sulfides A_xTiS_2, A_xNbS_2, and A_xTaS_2. *Inorg. Chem.* **1977**, *16*, 2950−2956.
(39) Schollhorn, R.; Meyer, H. Cathodic Reduction of Layered Transition-Metal Chalcogenides. *Mater. Res. Bull.* **1974**, *9*, 1237−1246.
(40) Chen, S. M. Preparation, Characterization, and Electrocatalytic Oxidation Properties of Iron, Cobalt, Nickel, and Indium Hexacyanoferrate. *J. Electroanal. Chem.* **2002**, *521*, 29−52.
(41) Wang, R. Y.; Wessells, C. D.; Huggins, R. A.; Cui, Y. Highly Reversible Open Framework Nanoscale Electrodes for Divalent Ion Batteries. *Nano Lett.* **2013**, *13*, 5748−5752.
(42) Hayashi, M.; Arai, H.; Ohtsuka, H.; Sakurai, Y. Electrochemical Characteristics of Calcium in Organic Electrolyte Solutions and Vanadium Oxides as Calcium Hosts. *J. Power Sources* **2003**, *119*, 617−620.
(43) Hayashi, M.; Arai, H.; Ohtsuka, H.; Sakurai, Y. Electrochemical Insertion/Extraction of Calcium Ions Using Crystalline Vanadium Oxide. *Electrochem. Solid-State Lett.* **2004**, *7*, A119−A121.
(44) Bervas, M.; Klein, L. C.; Amatucci, G. G. Vanadium Oxide-Propylene Carbonate Composite as a Host for the Intercalation of Polyvalent Cations. *Solid State Ionics* **2005**, *176*, 2735−2747.
(45) See, K. A.; Gerbec, J. A.; Jun, Y. S.; Wudl, F.; Stucky, G. D.; Seshadri, R. A High Capacity Calcium Primary Cell Based on the Ca-S System. *Adv. Energy Mater.* **2013**, *3*, 1056−1061.
(46) Kim, H.; Boysen, D. A.; Newhouse, J. M.; Spatocco, B. L.; Chung, B.; Burke, P. J.; Bradwell, D. J.; Jiang, K.; Tomaszowska, A. A.; Wang, K. L.; et al. Liquid Metal Batteries: Past, Present, and Future. *Chem. Rev.* **2013**, *113*, 2075−2099.
(47) Newhouse, J. M.; Poizeau, S.; Kim, H.; Spatocco, B. L.; Sadoway, D. R. Thermodynamic Properties of Calcium-Magnesium Alloys Determined by emf Measurements. *Electrochim. Acta* **2013**, *91*, 293−301.
(48) Kim, H.; Boysen, D. A.; Ouchi, T.; Sadoway, D. R. Calcium-Bismuth Electrodes for Large-Scale Energy Storage (Liquid Metal Batteries). *J. Power Sources* **2013**, *241*, 239−248.
(49) Ouchi, T.; Kim, H.; Ning, X. H.; Sadoway, D. R. Calcium-Antimony Alloys as Electrodes for Liquid Metal Batteries. *J. Electrochem. Soc.* **2014**, *161*, A1898−A1904.
(50) Poizeau, S.; Sadoway, D. R. Application of the Molecular Interaction Volume Model (MIVM) to Calcium-Based Liquid Alloys of Systems Forming High-Melting Intermetallics. *J. Am. Chem. Soc.* **2013**, *135*, 8260−8265.
(51) Ouchi, T.; Kim, H.; Spatocco, B. L.; Sadoway, D. R. Calcium-Based Multi-Element Chemistry for Grid-Scale Electrochemical Energy Storage. *Nat. Commun.* **2016**, *7*, 10999.
(52) Shiga, T.; Kondo, H.; Kato, Y.; Inoue, M. Insertion of Calcium Ion into Prussian Blue Analogue in Nonaqueous Solutions and Its Application to a Rechargeable Battery with Dual Carriers. *J. Phys. Chem. C* **2015**, *119*, 27946−27953.
(53) Padigi, P.; Goncher, G.; Evans, D.; Solanki, R. Potassium Barium Hexacyanoferrate - a Potential Cathode Material for Rechargeable Calcium Ion Batteries. *J. Power Sources* **2015**, *273*, 460−464.
(54) Tojo, T.; Sugiura, Y.; Inada, R.; Sakurai, Y. Reversible Calcium Ion Batteries Using a Dehydrated Prussian Blue Analogue Cathode. *Electrochim. Acta* **2016**, *207*, 22−27.
(55) Lipson, A. L.; Han, S. D.; Kim, S.; Pan, B. F.; Sa, N. Y.; Liao, C.; Fister, T. T.; Burrell, A. K.; Vaughey, J. T.; Ingram, B. J. Nickel Hexacyanoferrate, a Versatile Intercalation Host for Divalent Ions from Nonaqueous Electrolytes. *J. Power Sources* **2016**, *325*, 646−652.
(56) Rong, Z.; Malik, R.; Canepa, P.; Sai Gautam, G.; Liu, M.; Jain, A.; Persson, K.; Ceder, G. Materials Design Rules for Multivalent Ion Mobility in Intercalation Structures. *Chem. Mater.* **2015**, *27*, 6016−6021.
(57) Liu, M.; Rong, Z.; Malik, R.; Canepa, P.; Jain, A.; Ceder, G.; Persson, K. A. Spinel Compounds as Multivalent Battery Cathodes: A Systematic Evaluation Based on Ab Initio Calculations. *Energy Environ. Sci.* **2015**, *8*, 964−974.
(58) Ponrouch, A.; Tchitchekova, D.; Frontera, C.; Bardé, F.; Arroyo-de Dompablo, M. E.; Palacín, M. R. Assessing Si-Based Anodes for Ca-Ion Batteries: Electrochemical Decalciation of $CaSi_2$. *Electrochem. Commun.* **2016**, *66*, 75−78.
(59) Emery, N.; Herold, C.; Lagrange, P. Structural Study and Crystal Chemistry of the First Stage Calcium Graphite Intercalation Compound. *J. Solid State Chem.* **2005**, *178*, 2947−2952.
(60) Takeuchi, S.; Iriyama, Y.; Abe, T.; Ogumi, Z. Electrochemical Intercalation of Calcium Ion into Graphite Electrode. In *214th ECS Meeting*, Honolulu, HI, October 13, 2008; Abstract # 206.
(61) Tran, T. T.; Obrovac, M. N. Alloy Negative Electrodes for High Energy Density Metal-Ion Cells. *J. Electrochem. Soc.* **2011**, *158*, A1411−A1416.
(62) Gummow, R. J.; Vamvounis, G.; Kannan, M. B.; He, Y. H. Calcium-Ion Batteries: Current State-of-the-Art and Future Perspectives. *Adv. Mater.* **2018**, *30*, 1801702.
(63) Shiga, T.; Kato, Y.; Hase, Y. Coupling of Nitroxyl Radical as an Electrochemical Charging Catalyst and Ionic Liquid for Calcium Plating/Stripping toward a Rechargeable Calcium-Oxygen Battery. *J. Mater. Chem. A* **2017**, *5*, 13212−13219.
(64) Reinsberg, P.; Bondue, C. J.; Baltruschat, H. Calcium-Oxygen Batteries as a Promising Alternative to Sodium-Oxygen Batteries. *J. Phys. Chem. C* **2016**, *120*, 22179−22185.
(65) Tobias, C. W. *Advances in Electrochemistry and Electrochemical Engineering*; John Wiley & Sons Inc, 1967; Vol. *5*.
(66) Auborn, J. J.; French, K. W.; Lieberman, S. I.; Shah, V. K.; Heller, A. Lithium Anode Cells Operating at Room-Temperature in Inorganic Electrolytic Solutions. *J. Electrochem. Soc.* **1973**, *120*, 1613−1619.
(67) Behl, W. K.; Christopulos, J. A.; Ramirez, M.; Gilman, S. Lithium Inorganic Electrolyte Cells Utilizing Solvent Reduction. *J. Electrochem. Soc.* **1973**, *120*, 1619−1623.
(68) Peled, E.; Straze, H. Kinetics of Magnesium Electrode in Thionyl Chloride Solutions. *J. Electrochem. Soc.* **1977**, *124*, 1030−1035.
(69) Ellingham, H. J. T. Reducibility of Oxides and Sulfides in Metallurgical Processes. *J. Soc. Chem. Ind., London* **1944**, *63*, 125−133.
(70) Tucker, S. A.; Whitney, J. B. Some Observations on the Preparation of Metallic Calcium by Electrolysis. *J. Am. Chem. Soc.* **1906**, *28*, 84−87.
(71) Li, H.; Yin, H.; Wang, K.; Cheng, S.; Jiang, K.; Sadoway, D. R. Liquid Metal Electrodes for Energy Storage Batteries. *Adv. Energy Mater.* **2016**, *6*, 1600483.
(72) University of Cambridge. The Ellingham diagram in removal of contaminants. Dissemination of IT for the Promotion of Materials Science (DoITPoMS), TLP Library. https://www.doitpoms.ac.uk/tlplib/recycling-metals/ellingham.php (accessed March 15th, 2019).
(73) Wang, D.; Gao, X.; Chen, Y.; Jin, L.; Kuss, C.; Bruce, P. G. Plating and Stripping Calcium in an Organic Electrolyte. *Nat. Mater.* **2018**, *17*, 16−20.
(74) Ponrouch, A.; Frontera, C.; Barde, F.; Palacin, M. R. Towards a Calcium-Based Rechargeable Battery. *Nat. Mater.* **2016**, *15*, 169−172.

DOI: 10.1021/acs.chemrev.9b00339
Chem. Rev. 2020, 120, 6331−6357

(75) Ta, K.; Zhang, R.; Shin, M.; Rooney, R. T.; Neumann, E. K.; Gewirth, A. A. Understanding Ca Electrodeposition and Speciation Processes in Nonaqueous Electrolytes for Next-Generation Ca-Ion Batteries. *ACS Appl. Mater. Interfaces* **2019**, *11*, 21536−21542.
(76) Young, J. S.; Smeu, M. Ethylene Carbonate-Based Electrolyte Decomposition and Solid-Electrolyte Interphase Formation on Ca Metal Anodes. *J. Phys. Chem. Lett.* **2018**, *9*, 3295−3300.
(77) Ponrouch, A. Challenges and Opportunities in Interphased Ca Metal Anode Batteries. In *International Battery Association (IBA) Meeting*, San Diego, CA, March 2018.
(78) Shyamsunder, A.; Blanc, L. E.; Assoud, A.; Nazar, L. F. Reversible Calcium Plating and Stripping at Room Temperature Using a Borate Salt. *ACS Energy Lett.* **2019**, *4*, 2271−2276.
(79) Li, Z.; Fuhr, O.; Fichtner, M.; Zhao-Karger, Z. Towards Stable and Efficient Electrolytes for Room-Temperature Rechargeable Calcium Batteries. *Energy Environ. Sci.* **2019**; Advance Article.
(80) Yao, Z.; Hegde, V. I.; Aspuru-Guzik, A.; Wolverton, C. Discovery of Calcium-Metal Alloy Anodes for Reversible Ca-Ion Batteries. *Adv. Energy Mater.* **2019**, *9*, 1802994.
(81) Wu, N.; Yao, W.; Song, X.; Zhang, G.; Chen, B.; Yang, J.; Tang, Y. A Calcium-Ion Hybrid Energy Storage Device with High Capacity and Long Cycling Life under Room Temperature. *Adv. Energy Mater.* **2019**, *9*, 1803865.
(82) Wang, M.; Jiang, C. L.; Zhang, S. Q.; Song, X. H.; Tang, Y. B.; Cheng, H. M. Reversible Calcium Alloying Enables a Practical Room-Temperature Rechargeable Calcium-Ion Battery with a High Discharge Voltage. *Nat. Chem.* **2018**, *10*, 667−672.
(83) Keyzer, E. N.; Matthews, P. D.; Liu, Z.; Bond, A. D.; Grey, C. P.; Wright, D. S. Synthesis of $Ca(PF_6)_2$, Formed: Via Nitrosonium Oxidation of Calcium. *Chem. Commun.* **2017**, *53*, 4573−4576.
(84) Poizeau, S.; Kim, H.; Newhouse, J. M.; Spatocco, B. L.; Sadoway, D. R. Determination and Modeling of the Thermodynamic Properties of Liquid Calcium−Antimony Alloys. *Electrochim. Acta* **2012**, *76*, 8−15.
(85) Yin, H.; Wang, D. Electrolytic Germanium for Calcium Storage. *J. Electrochem. Soc.* **2016**, *163*, E351−E353.
(86) Deng, X.; Chen, X.; Huang, Y.; Xiao, B.; Du, H. Two-Dimensional GeP_3 as a High Capacity Anode Material for Non-Lithium-Ion Batteries. *J. Phys. Chem. C* **2019**, *123*, 4721−4728.
(87) Guerard, D.; Chaabouni, M.; Lagrange, P.; El Makrini, M.; Herold, A. Insertion De Metaux Alcalino-Terreux Dans Le Graphite. *Carbon* **1980**, *18*, 257−264.
(88) Srinivas, G.; Howard, C. A.; Bennington, S. M.; Skipper, N. T.; Ellerby, M. Effect of Hydrogenation on Structure and Superconducting Properties of CaC_6. *J. Mater. Chem.* **2009**, *19*, 5239−5243.
(89) Wu, S.; Zhang, F.; Tang, Y. A Novel Calcium-Ion Battery Based on Dual-Carbon Configuration with High Working Voltage and Long Cycling Life. *Adv. Sci.* **2018**, *5*, 1701082.
(90) Ishikawa, H.; Higuchi, H.; Kawaguchi, M. Intercalation of Calcium into a Graphite-Like Layered Material. *Chem. Lett.* **2018**, *47*, 891−893.
(91) Mortazavi, B.; Dianat, A.; Rahaman, O.; Cuniberti, G.; Rabczuk, T. Borophene as an Anode Material for Ca, Mg, Na or Li Ion Storage: A First-Principle Study. *J. Power Sources* **2016**, *329*, 456−461.
(92) Farokh Niaei, A. H.; Hussain, T.; Hankel, M.; Searles, D. J. Hydrogenated Defective Graphene as an Anode Material for Sodium and Calcium Ion Batteries: A Density Functional Theory Study. *Carbon* **2018**, *136*, 73−84.
(93) Datta, D.; Li, J.; Shenoy, V. B. Defective Graphene as a High-Capacity Anode Material for Na- and Ca-Ion Batteries. *ACS Appl. Mater. Interfaces* **2014**, *6*, 1788−1795.
(94) Er, D.; Li, J.; Naguib, M.; Gogotsi, Y.; Shenoy, V. B. Ti_3C_2 MXene as a High Capacity Electrode Material for Metal (Li, Na, K, Ca) Ion Batteries. *ACS Appl. Mater. Interfaces* **2014**, *6*, 11173−11179.
(95) Xie, Y.; Dall'Agnese, Y.; Naguib, M.; Gogotsi, Y.; Barsoum, M. W.; Zhuang, H. L.; Kent, P. R. C. Prediction and Characterization of MXene Nanosheet Anodes for Non-Lithium-Ion Batteries. *ACS Nano* **2014**, *8*, 9606−9615.
(96) Rodriguez-Perez, I. A.; Yuan, Y.; Bommier, C.; Wang, X.; Ma, L.; Leonard, D. P.; Lerner, M. M.; Carter, R. G.; Wu, T.; Greaney, P. A.; et al. Mg-Ion Battery Electrode: An Organic Solid's Herringbone Structure Squeezed Upon Mg-Ion Insertion. *J. Am. Chem. Soc.* **2017**, *139*, 13031−13037.
(97) Gheytani, S.; Liang, Y.; Wu, F.; Jing, Y.; Dong, H.; Rao, K. K.; Chi, X.; Fang, F.; Yao, Y. An Aqueous Ca-Ion Battery. *Adv. Sci.* **2017**, *4*, 1700465.
(98) Yin, H.; Xiao, W.; Mao, X.; Zhu, H.; Wang, D. Preparation of a Porous Nanostructured Germanium from GeO_2 Via a "Reduction−Alloying−Dealloying" Approach. *J. Mater. Chem. A* **2015**, *3*, 1427−1430.
(99) Jow, R. T.; Xu, K.; Borodin, O.; Ue, M., Eds. *Electrolytes for Lithium and Lithium Ion Batteries*; Springer: New York, 2014.
(100) Lipson, A. L.; Pan, B. F.; Lapidus, S. H.; Liao, C.; Vaughey, J. T.; Ingram, B. J. Rechargeable Ca-Ion Batteries: A New Energy Storage System. *Chem. Mater.* **2015**, *27*, 8442−8447.
(101) Tchitchekova, D. S.; Monti, D.; Johansson, P.; Barde, F.; Randon-Vitanova, A.; Palacin, M. R.; Ponrouch, A. On the Reliability of Half-Cell Tests for Monovalent (Li^+, Na^+) and Divalent (Mg^{2+}, Ca^{2+}) Cation Based Batteries. *J. Electrochem. Soc.* **2017**, *164*, A1384−A1392.
(102) Sa, N. Y.; Wang, H.; Proffit, D. L.; Lipson, A. L.; Key, B.; Liu, M.; Feng, Z. X.; Fister, T. T.; Ren, Y.; Sun, C. J.; et al. Is alpha-V_2O_5 a Cathode Material for Mg Insertion Batteries? *J. Power Sources* **2016**, *323*, 44−50.
(103) Hardwick, L. J.; de Leon, C. P. Rechargeable Multi-Valent Metal-Air Batteries a Review of Research and Current Challenges in Secondary Multivalent Metal-Oxygen Batteries. *Johnson Matthey Technol. Rev.* **2018**, *62*, 134−149.
(104) Suo, L.; Borodin, O.; Gao, T.; Olguin, M.; Ho, J.; Fan, X.; Luo, C.; Wang, C.; Xu, K. Water-in-Salt" Electrolyte Enables High-Voltage Aqueous Lithium-Ion Chemistries. *Science* **2015**, *350*, 938−943.
(105) Lee, C.; Jeong, S.-K. A Novel Superconcentrated Aqueous Electrolyte to Improve the Electrochemical Performance of Calcium-Ion Batteries. *Chem. Lett.* **2016**, *45*, 1447−1449.
(106) Lee, C.; Jeong, S.-K. Modulating the Hydration Number of Calcium Ions by Varying the Electrolyte Concentration: Electrochemical Performance in a Prussian Blue Electrode/Aqueous Electrolyte System for Calcium-Ion Batteries. *Electrochim. Acta* **2018**, *265*, 430−436.
(107) Kim, H.; Boysen, D. A.; Bradwell, D. J.; Chung, B.; Jiang, K.; Tomaszowska, A. A.; Wang, K.; Wei, W.; Sadoway, D. R. Thermodynamic Properties of Calcium−Bismuth Alloys Determined by Emf Measurements. *Electrochim. Acta* **2012**, *60*, 154−162.
(108) Lu, Z.; Ciucci, F. Metal Borohydrides as Electrolytes for Solid-State Li, Na, Mg, and Ca Batteries: A First-Principles Study. *Chem. Mater.* **2017**, *29*, 9308−9319.
(109) Bakker, A.; Gejji, S.; Lindgren, J.; Hermansson, K. M.Probst, M. Contact Ion Pair Formation and Ether Oxygen Coordination in the Polymer Electrolytes $M[N(CF_3SO_2)_2]_2$peon for M = Mg, Ca, Sr and Ba. *Polymer* **1995**, *36*, 4371−4378.
(110) Genier, F. S.; Burdin, C. V.; Biria, S.; Hosein, I. D. A Novel Calcium-Ion Solid Polymer Electrolyte Based on Crosslinked Poly-(Ethylene Glycol) Diacrylate. *J. Power Sources* **2019**, *414*, 302−307.
(111) Kortan, A. R.; Kopylov, N.; Glarum, S.; Gyorgy, E. M.; Ramirez, A. P.; Fleming, R. M.; Thiel, F. A.; Haddon, R. C. Superconductivity at 8.4-K in Calcium-Doped C60. *Nature* **1992**, *355*, 529−532.
(112) Levi, E.; Gershinsky, G.; Aurbach, D.; Isnard, O.; Ceder, G. New Insight on the Unusually High Ionic Mobility in Chevrel Phases. *Chem. Mater.* **2009**, *21*, 1390−1399.
(113) Lukatskaya, M. R.; Mashtalir, O.; Ren, C. E.; Dall'Agnese, Y.; Rozier, P.; Taberna, P. L.; Naguib, M.; Simon, P.; Barsoum, M. W.; Gogotsi, Y. Cation Intercalation and High Volumetric Capacitance of Two-Dimensional Titanium Carbide. *Science* **2013**, *341*, 1502−1505.
(114) Murphy, D. W. Insertion Reactions in Electrode Materials. *Solid State Ionics* **1986**, *18−19*, 847−851.
(115) Goodenough, J. B.; Park, K.-S. The Li-Ion Rechargeable Battery: A Perspective. *J. Am. Chem. Soc.* **2013**, *135*, 1167−1176.
(116) Etacheri, V.; Marom, R.; Elazari, R.; Salitra, G.; Aurbach, D. Challenges in the Development of Advanced Li-Ion Batteries: A Review. *Energy Environ. Sci.* **2011**, *4*, 3243−3262.

DOI: 10.1021/acs.chemrev.9b00339
Chem. Rev. 2020, 120, 6331−6357

(117) Whittingham, M. S. Lithium Batteries and Cathode Materials. *Chem. Rev.* **2004**, *104*, 4271−4301.
(118) Tarascon, J. M.; Armand, M. Issues and Challenges Facing Rechargeable Lithium Batteries. *Nature* **2001**, *414*, 359−367.
(119) Ling, C.; Chen, J. J.; Mizuno, F. First-Principles Study of Alkali and Alkaline Earth Ion Intercalation in Iron Hexacyanoferrate: The Important Role of Ionic Radius. *J. Phys. Chem. C* **2013**, *117*, 21158−21165.
(120) Gautam, G. S.; Canepa, P.; Malik, R.; Liu, M.; Persson, K.; Ceder, G. First-Principles Evaluation of Multi-Valent Cation Insertion into Orthorhombic V_2O_5. *Chem. Commun.* **2015**, *51*, 13619−13622.
(121) Liu, M.; Jain, A.; Rong, Z.; Qu, X.; Canepa, P.; Malik, R.; Ceder, G.; Persson, K. A. Evaluation of Sulfur Spinel Compounds for Multivalent Battery Cathode Applications. *Energy Environ. Sci.* **2016**, *9*, 3201−3209.
(122) Ling, C.; Mizuno, F. Phase Stability of Post-Spinel Compound AMn_2O_4 (a = Li, Na, or Mg) and Its Application as a Rechargeable Battery Cathode. *Chem. Mater.* **2013**, *25*, 3062−3071.
(123) Carrasco, J. Role of Van Der Waals Forces in Thermodynamics and Kinetics of Layered Transition Metal Oxide Electrodes: Alkali and Alkaline-Earth Ion Insertion into V_2O_5. *J. Phys. Chem. C* **2014**, *118*, 19599−19607.
(124) Tchitchekova, D. S.; Ponrouch, A.; Verrelli, R.; Broux, T.; Frontera, C.; Sorrentino, A.; Barde, F.; Biskup, N.; Arroyo-de Dompablo, M. E.; Palacin, M. R. Electrochemical Intercalation of Calcium and Magnesium in TiS_2: Fundamental Studies Related to Multivalent Battery Applications. *Chem. Mater.* **2018**, *30*, 847−856.
(125) Verrelli, R.; Black, A. P.; Pattanathummasid, C.; Tchitchekova, D. S.; Ponrouch, A.; Oro-Sole, J.; Frontera, C.; Barde, F.; Rozier, P.; Palacin, M. R. On the Strange Case of Divalent Ions Intercalation in V_2O_5. *J. Power Sources* **2018**, *407*, 162−172.
(126) Parija, A.; Liang, Y.; Andrews, J. L.; De Jesus, L. R.; Prendergast, D.; Banerjee, S. Topochemically De-Intercalated Phases of V_2O_5 as Cathode Materials for Multivalent Intercalation Batteries: A First-Principles Evaluation. *Chem. Mater.* **2016**, *28*, 5611−5620.
(127) Recham, N.; Rousse, G.; Sougrati, M. T.; Chotard, J.-N.; Frayret, C.; Mariyappan, S.; Melot, B. C.; Jumas, J.-C.; Tarascon, J.-M. Preparation and Characterization of a Stable $FeSO_4F$-Based Framework for Alkali Ion Insertion Electrodes. *Chem. Mater.* **2012**, *24*, 4363−4370.
(128) Radin, M. D.; Van der Ven, A. Stability of Prismatic and Octahedral Coordination in Layered Oxides and Sulfides Intercalated with Alkali and Alkaline-Earth Metals. *Chem. Mater.* **2016**, *28*, 7898−7904.
(129) Ceder, G. Computational Materials Science - Predicting Properties from Scratch. *Science* **1998**, *280*, 1099−1100.
(130) Meng, Y. S.; Arroyo-de Dompablo, M. E. First Principles Computational Materials Design for Energy Storage Materials in Lithium Ion Batteries. *Energy Environ. Sci.* **2009**, *2*, 589−609.
(131) Juran, T. R.; Smeu, M. Hybrid Density Functional Theory Modeling of Ca, Zn, and Al Ion Batteries Using the Chevrel Phase Mo_6S_8 Cathode. *Phys. Chem. Chem. Phys.* **2017**, *19*, 20684−20690.
(132) Arroyo-de Dompablo, M. E.; Krich, C.; Nava-Avendano, J.; Palacin, M. R.; Barde, F. In Quest of Cathode Materials for Ca Ion Batteries: The $CaMO_3$ Perovskites (M = Mo, Cr, Mn, Fe, Co, and Ni). *Phys. Chem. Chem. Phys.* **2016**, *18*, 19966−19972.
(133) Zhang, Z.; Zhang, X.; Zhao, X.; Yao, S.; Chen, A.; Zhou, Z. Computational Screening of Layered Materials for Multivalent Ion Batteries. *ACS Omega* **2019**, *4*, 7822−7828.
(134) Arroyo-de Dompablo, M. E.; Krich, C.; Nava-Avendano, J.; Biskup, N.; Palacin, M. R.; Barde, F. A Joint Computational and Experimental Evaluation of $CaMn_2O_4$ Polymorphs as Cathode Materials for Ca Ion Batteries. *Chem. Mater.* **2016**, *28*, 6886−6893.
(135) Shannon, R. D.; Prewitt, C. T. Effective Ionic Radii in Oxides and Fluorides. *Acta Crystallogr., Sect. B: Struct. Crystallogr. Cryst. Chem.* **1969**, *25*, 925−946.
(136) Manthiram, A. Materials Aspect: An Overview. *Lithium Batteries* **2003**, 3−41.
(137) Croguennec, L.; Palacin, M. R. Recent Achievements on Inorganic Electrode Materials for Lithium-Ion Batteries. *J. Am. Chem. Soc.* **2015**, *137*, 3140−3156.
(138) Thackeray, M. M.; Johnson, P. J.; De Picciotto, L. A.; Bruce, P. G.; Goodenough, J. B. Electrochemical Extraction of Lithium from $LiMn_2O_4$. *Mater. Res. Bull.* **1984**, *19*, 179−187.
(139) Gaudefroy, C.; Jouravsky, G.; Permingeat, F. La Marokite, $CaMn_2O_4$, Une Nouvelle EsÞEce MińErale. *Bull. Soc. Fr. Mineral. Cristallogr.* **1963**, *86*, 359−367.
(140) Brese, N. E.; O'Keeffe, M. Crystal-Chemistry of Inorganic Nitrides. *Struct. Bonding (Berlin)* **1992**, *79*, 307−378.
(141) Chern, M. Y.; Disalvo, F. J. Synthesis, Structure, Electric, and Magnetic-Properties of CaNiN. *J. Solid State Chem.* **1990**, *88*, 459−464.
(142) Laurent, Y.; Lang, J. Combinaisons du nitrure de silicium avec le nitrure de calcium. *C. R. Seances Acad. Sci., Ser. C* **1966**, *262*, 340.
(143) Shannon, R. D. Revised Effective Ionic-Radii and Systematic Studies of Interatomic Distances in Halides and Chalcogenides. *Acta Crystallogr., Sect. A: Cryst. Phys., Diffr., Theor. Gen. Crystallogr.* **1976**, *32*, 751−767.
(144) Rosenberg, M.; Nicolau, P. Electrical Properties and Cation Migration in $MgMn_2O_4$. *Phys. Status Solidi B* **1964**, *6*, 101−110.
(145) Okamoto, S.; Ichitsubo, T.; Kawaguchi, T.; Kumagai, Y.; Oba, F.; Yagi, S.; Shimokawa, K.; Goto, N.; Doi, T.; Matsubara, E. Intercalation and Push-out Process with Spinel-to-Rocksalt Transition on Mg Insertion into Spinel Oxides in Magnesium Batteries. *Adv. Sci.* **2015**, *2*, 1500072.
(146) Knight, J. C.; Therese, S.; Manthiram, A. On the Utility of Spinel Oxide Hosts for Magnesium-Ion Batteries. *ACS Appl. Mater. Interfaces* **2015**, *7*, 22953−22961.
(147) Sai Gautam, G.; Canepa, P.; Urban, A.; Bo, S.-H.; Ceder, G. Influence of Inversion on Mg Mobility and Electrochemistry in Spinels. *Chem. Mater.* **2017**, *29*, 7918−7930.
(148) Brown, G. E. Olivines and Silicate Spinels. *Reviews in Mineralogy; Orthosilicates* **1982**, *5*, 275−382.
(149) Morgan, D.; Van der Ven, A.; Ceder, G. Li Conductivity in Li_xMPO_4 (M = Mn, Fe, Co, Ni) Olivine Materials. *Electrochem. Solid-State Lett.* **2004**, *7*, A30−A32.
(150) Padhi, A. K.; Nanjundaswamy, K. S.; Goodenough, J. B. Phospho-Olivines as Positive-Electrode Materials for Rechargeable Lithium Batteries. *J. Electrochem. Soc.* **1997**, *144*, 1188−1194.
(151) Redfern, S. A. T.; Artioli, G.; Rinaldi, R.; Henderson, C. M. B.; Knight, K. S.; Wood, B. J. Octahedral Cation Ordering in Olivine at High Temperature. Ii: An in Situ Neutron Powder Diffraction Study on Synthetic $MgFeSiO_4$ (Fa50). *Phys. Chem. Miner.* **2000**, *27*, 630−637.
(152) Francis, C. A.; Ribbe, P. H. The Forsterite-Tephroite Series: I. Crystal-Structure Refinements. *Am. Mineral.* **1980**, *65*, 1263−1269.
(153) Folco, L.; Mellini, M. Crystal Chemistry of Meteoritic Kirschsteinite. *Eur. J. Mineral.* **1997**, *9*, 969−973.
(154) Torres, A.; Luque, F. J.; Tortajada, J.; Arroyo de Dompablo, M. E. Analysis of Minerals as Cathode Materials for Ca-Based Rechargeable Batteries. *Sci. Rep.* **2019**, *9*, 9644.
(155) Goldschmidt, V. M. The Principles of Distribution of Chemical Elements in Minerals and Rocks. The Seventh Hugo Muller Lecture, Delivered before the Chemical Society on March 17th, 1937. *J. Chem. Soc.* **1937**, *0*, 655−673.
(156) Ohzuku, T.; Ueda, A.; Nagayama, M.; Iwakoshi, Y.; Komori, H. Comparative-Study of $LiCoO_2$, $Lini_{1/2}Co_{1/2}O_2$ and $LiNio_2$ for 4-V Secondary Lithium Cells. *Electrochim. Acta* **1993**, *38*, 1159−1167.
(157) Ohzuku, T.; Ueda, A. Solid-State Redox Reactions of $LiCoO_2$ (R-3m) for 4 V Secondary Lithium Cells. *J. Electrochem. Soc.* **1994**, *141*, 2972−2977.
(158) Mizushima, K.; Jones, P. C.; Wiseman, P. J.; Goodenough, J. B. Li_xCoO_2 ($0< x \leq 1$)- a New Cathode Material for Batteries of High-Energy Density. *Mater. Res. Bull.* **1980**, *15*, 783−789.
(159) Berthelot, R.; Carlier, D.; Delmas, C. Electrochemical Investigation of the P2-Na_xCoO_2 Phase Diagram. *Nat. Mater.* **2011**, *10*, 74−80.
(160) Yabuuchi, N.; Kajiyama, M.; Iwatate, J.; Nishikawa, H.; Hitomi, S.; Okuyama, R.; Usui, R.; Yamada, Y.; Komaba, S. P2-Type

DOI: 10.1021/acs.chemrev.9b00339
Chem. Rev. 2020, 120, 6331−6357

$Na_xFe_{1/2}Mn_{1/2}O_2$ Made from Earth-Abundant Elements for Rechargeable Na Batteries. *Nat. Mater.* **2012**, *11*, 512−517.
(161) Varela, A.; de Dios, S.; Parras, M.; Hernando, M.; Fernandez-Diaz, M. T.; Landa-Canovas, A. R.; Gonzalez-Calbet, J. M. Ordered Rock-Salt Related Nanoclusters in $CaMnO_2$. *J. Am. Chem. Soc.* **2009**, *131*, 8660−8668.
(162) Miyazaki, Y.; Huang, X. Y.; Kajiwara, T.; Yamane, H.; Kajitani, T. Synthesis, Crystal Structure and Physical Properties of Layered Cobalt Oxide Ca_xCoO_2 ($x \sim 0.47$). *J. Ceram. Soc. Jpn.* **2009**, *117*, 42−46.
(163) Woermann, E.; Muan, A. Phase Equilibria in System Cao-Cobalt Oxide in Air. *J. Inorg. Nucl. Chem.* **1970**, *32*, 1455−1459.
(164) Cabello, M.; Nacimiento, F.; González, J. R.; Ortiz, G.; Alcántara, R.; Lavela, P.; Pérez-Vicente, C.; Tirado, J. L. Advancing Towards a Veritable Calcium-Ion Battery: $CaCo_2O_4$ Positive Electrode Material. *Electrochem. Commun.* **2016**, *67*, 59−64.
(165) Seo, D.-H.; Lee, J.; Urban, A.; Malik, R.; Kang, S.; Ceder, G. The Structural and Chemical Origin of the Oxygen Redox Activity in Layered and Cation-Disordered Li-Excess Cathode Materials. *Nat. Chem.* **2016**, *8*, 692−697.
(166) Fell, C. R.; Lee, D. H.; Meng, Y. S.; Gallardo-Amores, J. M.; Moran, E.; Arroyo-de Dompablo, M. E. High Pressure Driven Structural and Electrochemical Modifications in Layered Lithium Transition Metal Intercalation Oxides. *Energy Environ. Sci.* **2012**, *5*, 6214−6224.
(167) Breger, J.; Dupre, N.; Chupas, P. J.; Lee, P. L.; Proffen, T.; Parise, J. B.; Grey, C. P. Short- and Long-Range Order in the Positive Electrode Material, $Li(NiMn)_{0.5}O_2$: A Joint X-Ray and Neutron Diffraction, Pair Distribution Function Analysis and Nmr Study. *J. Am. Chem. Soc.* **2005**, *127*, 7529−7537.
(168) Murphy, D. W.; Disalvo, F. J.; Hull, G. W.; Waszczak, J. V. Convenient Preparation and Physical-Properties of Lithium Intercalation Compounds of Group-4b and Group-5b Layered Transition-Metal Dichalcogenides. *Inorg. Chem.* **1976**, *15*, 17−21.
(169) Julien, C. M. Lithium Intercalated Compounds - Charge Transfer and Related Properties. *Mater. Sci. Eng., R* **2003**, *40*, 47−102.
(170) Murata, Y.; Takada, S.; Obata, T.; Tojo, T.; Inada, R.; Sakurai, Y. Effect of Water in Electrolyte on the Ca^{2+} Insertion/Extraction Properties of V_2O_5. *Electrochim. Acta* **2019**, *294*, 210−216.
(171) Delmas, C.; Cognacauradou, H.; Cocciantelli, J. M.; Menetrier, M.; Doumerc, J. P. The $Li_xV_2O_5$ System - an Overview of the Structure Modifications Induced by the Lithium Intercalation. *Solid State Ionics* **1994**, *69*, 257−264.
(172) Uchaker, E.; Zheng, Y. Z.; Li, S.; Candelaria, S. L.; Hu, S.; Cao, G. Z. Better Than Crystalline: Amorphous Vanadium Oxide for Sodium-Ion Batteries. *J. Mater. Chem. A* **2014**, *2*, 18208−18214.
(173) Deng, L.; Niu, X.; Ma, G.; Yang, Z.; Zeng, L.; Zhu, Y.; Guo, L. Layered Potassium Vanadate $K_{0.5}V_2O_5$ as a Cathode Material for Nonaqueous Potassium Ion Batteries. *Adv. Funct. Mater.* **2018**, *28*, 1800670.
(174) Umrigar, C.; Ellis, D. E.; Wang, D.; Krakauer, H.; Posternak, M. Band-Structure, Intercalation, and Interlayer Interactions of Transition-Metal Dichalcogenides - TiS_2 and $LiTiS_2$. *Phys. Rev. B: Condens. Matter Mater. Phys.* **1982**, *26*, 4935−4950.
(175) Thompson, A. H. Lithium Ordering in Li_xTiS_2. *Phys. Rev. Lett.* **1978**, *40*, 1511−1514.
(176) Lee, C.; Jeong, Y.-T.; Nogales, P. M.; Song, H.-Y.; Kim, Y.; Yin, R.-Z.; Jeong, S.-K. Electrochemical Intercalation of Ca^{2+} Ions into TiS_2 in Organic Electrolytes at Room Temperature. *Electrochem. Commun.* **2019**, *98*, 115−118.
(177) Rouxel, J. Ionicity-Structure Diagram for Alkaline Intercalary Compounds of Lamellar Sulfides. *J. Solid State Chem.* **1976**, *17*, 223−229.
(178) Hibma, T. Structural Aspects of Monovalent Cation Intercalates of Layered Dichalcogenides. *Intercalation Chemistry* **1982**, 285−313.
(179) Aydinol, M. K.; Kohan, A. F.; Ceder, G.; Cho, K.; Joannopoulos, J. Ab Initio Study of Lithium Intercalation in Metal Oxides and Metal Dichalcogenides. *Phys. Rev. B: Condens. Matter Mater. Phys.* **1997**, *56*, 1354−1365.
(180) Goodenough, J. B.; Kim, Y. Challenges for Rechargeable Li Batteries. *Chem. Mater.* **2010**, *22*, 587−603.
(181) Nanjundaswamy, K. S.; Padhi, A. K.; Goodenough, J. B.; Okada, S.; Ohtsuka, H.; Arai, H.; Yamaki, J. Synthesis, Redox Potential Evaluation and Electrochemical Characteristics of Nasicon-Related-3D Framework Compounds. *Solid State Ionics* **1996**, *92*, 1−10.
(182) Smeu, M.; Hossain, M. S.; Wang, Z.; Timoshevskii, V.; Bevan, K. H.; Zaghib, K. Theoretical Investigation of Chevrel Phase Materials for Cathodes Accommodating Ca^{2+} Ions. *J. Power Sources* **2016**, *306*, 431−436.
(183) Bardé, F.; Palacin, M. R.; Stoytcheva, D.; Ponrouch, A.; Arroyo de Dompablo, M. E.; Biskup, N. Titanium-Based Positive Electrode Materials for Rechargeable Calcium Batteries and Cell Comprising the Same. WO2018197021, 2018.
(184) Torres, A.; Luque, F. J.; Tortajada, J.; Arroyo de Dompablo, M. E. DFT Investigation of Ca Mobility in Reduced-Perovskite and Oxidized- Marokite Oxides. *Energy Storage Materials* **2019**, *21*, 354−360.
(185) Torres, A.; Bardé, F.; Arroyo-de Dompablo, M. E. Evaluation of Cobalt Oxides for Calcium Battery Cathode Applications. *Solid State Ionics* **2019**, *340*, 115004.
(186) Padhi, A. K.; Nanjundaswamy, K. S.; Masquelier, C.; Goodenough, J. B. Mapping of Transition Metal Redox Energies in Phosphates with Nasicon Structure by Lithium Intercalation. *J. Electrochem. Soc.* **1997**, *144*, 2581−2586.
(187) Tchitchekova, D. S.; Frontera, C.; Ponrouch, A.; Krich, C.; Barde, F.; Palacin, M. R. Electrochemical Calcium Extraction from 1D-$Ca_3Co_2O_6$. *Dalton Transactions* **2018**, *47*, 11298−11302.
(188) Cabello, M.; Nacimiento, F.; Alcantara, R.; Lavela, P.; Perez Vicente, C.; Tirado, J. L. Applicability of Molybdite as an Electrode Material in Calcium Batteries: A Structural Study of Layer-Type Ca_xMoO3. *Chem. Mater.* **2018**, *30*, 5853−5861.
(189) Nyten, A.; Abouimrane, A.; Armand, M.; Gustafsson, T.; Thomas, J. O. Electrochemical Performance of Li_2FeSiO_4 as a New Li-Battery Cathode Material. *Electrochem. Commun.* **2005**, *7*, 156−160.
(190) Arroyo-de Dompablo, M. E.; Armand, M.; Tarascon, J. M.; Amador, U. On-Demand Design of Polyoxianionic Cathode Materials Based on Electronegativity Correlations: An Exploration of the Li_2MSiO_4 System (M = Fe, Mn, Co, Ni). *Electrochem. Commun.* **2006**, *8*, 1292−1298.
(191) Dominko, R.; Bele, M.; Gaberscek, M.; Meden, A.; Remskar, M.; Jamnik, J. Structure and Electrochemical Performance of Li_2MnSiO_4 and Li_2FeSiO_4 as Potential Li-Battery Cathode Materials. *Electrochem. Commun.* **2006**, *8*, 217−222.
(192) Saracibar, A.; Wang, Z.; Carroll, K. J.; Meng, Y. S.; Arroyo-de Dompablo, M. E. New Insights into the Electrochemical Performance of Li_2MnSiO_4: Effect of Cationic Substitutions. *J. Mater. Chem. A* **2015**, *3*, 6004−6011.
(193) Radin, M. D.; Alvarado, J.; Meng, Y. S.; Van der Ven, A. Role of Crystal Symmetry in the Reversibility of Stacking-Sequence Changes in Layered Intercalation Electrodes. *Nano Lett.* **2017**, *17*, 7789−7795.
(194) Lipson, A. L.; Kim, S.; Pan, B.; Liao, C.; Fister, T. T.; Ingram, B. J. Calcium Intercalation into Layered Fluorinated Sodium Iron Phosphate. *J. Power Sources* **2017**, *369*, 133−137.
(195) Fjellvag, H.; Gulbrandsen, E.; Aasland, S.; Olsen, A.; Hauback, B. C. Crystal Structure and Possible Charge Ordering in One-Dimensional $Ca_3Co_2O_6$. *J. Solid State Chem.* **1996**, *124*, 190−194.
(196) Boulahya, K.; Parras, M.; Gonzalez-Calbet, J. M. The $A_{(n+2)}B_{(n)}B'O_{(3n+3)}$ family (B = B '=Co): Ordered Intergrowth between 2H-$BaCoO_3$ and $Ca_3Co_2O_6$ Structures. *J. Solid State Chem.* **1999**, *145*, 116−127.
(197) Torres, A.; Arroyo-de Dompablo, M. E. Comparative Investigation of $MgMnSiO_4$ and Olivine-Type $MgMnSiS_4$ as Cathode Materials for Mg Batteries. *J. Phys. Chem. C* **2018**, *122*, 9356−9362.
(198) Sheppard, D.; Xiao, P.; Chemelewski, W.; Johnson, D. D.; Henkelman, G. A Generalized Solid-State Nudged Elastic Band Method. *J. Chem. Phys.* **2012**, *136*, 074103.

DOI: 10.1021/acs.chemrev.9b00339
Chem. Rev. 2020, 120, 6331−6357

(199) Millet, P.; Satto, C.; Sciau, P.; Galy, J. MgV_2O_5 and delta-$Li_xV_2O_5$: A Comparative Structural Investigation. *J. Solid State Chem.* **1998**, *136*, 56−62.
(200) Juran, T. R.; Smeu, M. $TiSe_2$ Cathode for Beyond Li-Ion Batteries. *J. Power Sources* **2019**, *436*, 226813.
(201) Verrelli, R.; Black, A. P.; Frontera, C.; Oro-Sole, J.; Arroyo-de Dompablo, M. E.; Fuertes, A.; Palacin, M. R. On the Study of Ca and Mg Deintercalation from Ternary Tantalum Nitrides. *ACS Omega* **2019**, *4*, 8943−8952.
(202) Knauth, P. Inorganic Solid Li Ion Conductors: An Overview. *Solid State Ionics* **2009**, *180*, 911−916.
(203) Thangadurai, V.; Narayanan, S.; Pinzaru, D. Garnet-Type Solid-State Fast Li Ion Conductors for Li Batteries: Critical Review. *Chem. Soc. Rev.* **2014**, *43*, 4714−4727.
(204) Liang, Y. L.; Tao, Z. L.; Chen, J. Organic Electrode Materials for Rechargeable Lithium Batteries. *Adv. Energy Mater.* **2012**, *2*, 742−769.
(205) Song, Z.; Zhou, H. Towards Sustainable and Versatile Energy Storage Devices: An Overview of Organic Electrode Materials. *Energy Environ. Sci.* **2013**, *6*, 2280−2301.
(206) Zhao, Q.; Lu, Y.; Chen, J. Advanced Organic Electrode Materials for Rechargeable Sodium-Ion Batteries. *Adv. Energy Mater.* **2017**, *7*, 1601792.
(207) Chen, H.; Armand, M.; Demailly, G.; Dolhem, F.; Poizot, P.; Tarascon, J.-M. From Biomass to a Renewable $Li_xC_6O_6$ Organic Electrode for Sustainable Li-Ion Batteries. *ChemSusChem* **2008**, *1*, 348−355.
(208) Poizot, P.; Dolhem, F.; Gaubicher, J. Progress in All-Organic Rechargeable Batteries Using Cationic and Anionic Configurations: Toward Low-Cost and Greener Storage Solutions? *Curr. Opin. Electrochem.* **2018**, *9*, 70−80.
(209) Novak, P.; Muller, K.; Santhanam, K. S. V.; Haas, O. Electrochemically Active Polymers for Rechargeable Batteries. *Chem. Rev.* **1997**, *97*, 207−281.
(210) Yu, X. W.; Manthiram, A. Ambient-Temperature Energy Storage with Polyvalent Metal-Sulfur Chemistry. *Small Methods* **2017**, *1*, 1700217.
(211) Bruce, P. G.; Freunberger, S. A.; Hardwick, L. J.; Tarascon, J. M. Li−O_2 and Li−S Batteries with High Energy Storage. *Nat. Mater.* **2012**, *11*, 19−29.
(212) Izustu, K. *Electrochemistry in Nonaqueous Solutions*; Wiley-VCH Verlag GmbH, 2002.
(213) Demir-Cakan, R.; Palacin, M. R.; Croguennec, L. Rechargeable aqueous electrolyte batteries: from univalent to multivalent cation chemistry. *J. Mater. Chem. A* **2019**, *7*, 20519−20539.
(214) Pecher, O.; Carretero-Gonzalez, J.; Griffith, K. J.; Grey, C. P. Materials' Methods: NMR in Battery Research. *Chem. Mater.* **2017**, *29*, 213−242.
(215) Grey, C. P.; Tarascon, J. M. Sustainability and in Situ Monitoring in Battery Development. *Nat. Mater.* **2017**, *16*, 45−56.
(216) Nelson, J.; Misra, S.; Yang, Y.; Jackson, A.; Liu, Y.; Wang, H.; Dai, H.; Andrews, J. C.; Cui, Y.; Toney, M. F. In Operando X-Ray Diffraction and Transmission X-Ray Microscopy of Lithium Sulfur Batteries. *J. Am. Chem. Soc.* **2012**, *134*, 6337−6343.
(217) Shao-Horn, Y. Understanding Phase Transformations in Lithium Battery Materials by Transmission Electron Microscopy. *Lithium Batteries* **2003**, 478−503.
(218) Conder, J.; Bouchet, R.; Trabesinger, S.; Marino, C.; Gubler, L.; Villevieille, C. Direct Observation of Lithium Polysulfides in Lithium-Sulfur Batteries Using Operando X-Ray Diffraction. *Nat. Energy* **2017**, *2*, 17069.
(219) Lipson, A. L.; Proffit, D. L.; Pan, B. F.; Fister, T. T.; Liao, C.; Burrell, A. K.; Vaughey, J. T.; Ingram, B. J. Current Collector Corrosion in Ca-Ion Batteries. *J. Electrochem. Soc.* **2015**, *162*, A1574−A1578.
(220) Wang, H.; Senguttuvan, P.; Proffit, D. L.; Pan, B. F.; Liao, C.; Burrell, A. K.; Vaughey, J. T.; Key, B. Formation of MgO During Chemical Magnesiation of Mg-Ion Battery Materials. *ECS Electrochem. Lett.* **2015**, *4*, A90−A93.
(221) Proffit, D. L.; Fister, T. T.; Kim, S.; Pan, B.; Liao, C.; Vaughey, J. T. Utilization of Ca K-Edge X-Ray Absorption Near Edge Structure to Identify Intercalation in Potential Multivalent Battery Materials. *J. Electrochem. Soc.* **2016**, *163*, A2508−A2514.
(222) Bouloux, J. C.; Galy, J. Alkaline-Earth Hypovanadates - Structural Evolution of CaV_nO_{2n+1} Series (n = 1,2,3,4). *J. Solid State Chem.* **1976**, *16*, 385−391.
(223) Onoda, M.; Nishiguchi, N. Crystal Structure and Spin Gap State of CaV_2O_5. *J. Solid State Chem.* **1996**, *127*, 359−362.
(224) Ceder, G.; Van der Ven, A. Phase Diagrams of Lithium Transition Metal Oxides: Investigations from First Principles. *Electrochim. Acta* **1999**, *45*, 131−150.
(225) Monti, D.; Ponrouch, A.; Araujo, R. B.; Barde, F.; Johansson, P.; Palacin, M. R. Multivalent Batteries - Prospects for High Energy Density: Ca Batteries. *Front. Chem.* **2019**, *7*, 79.
(226) Berg, E. J.; Villevieille, C.; Streich, D.; Trabesinger, S.; Novak, P. Rechargeable Batteries: Grasping for the Limits of Chemistry. *J. Electrochem. Soc.* **2015**, *162*, A2468−A2475.
(227) Vo, T. N.; Kim, H.; Hur, J.; Choi, W.; Kim, I. T. Surfactant-Assisted Ammonium Vanadium Oxide as a Superior Cathode for Calcium-Ion Batteries. *J. Mater. Chem. A* **2018**, *6*, 22645−22654.
(228) Tojo, T.; Tawa, H.; Oshida, N.; Inada, R.; Sakurai, Y. Electrochemical Characterization of a Layered alpha-MoO_3 as a New Cathode Material for Calcium Ion Batteries. *J. Electroanal. Chem.* **2018**, *825*, 51−56.
(229) Hyoung, J.; Heo, J. W.; Hong, S.-T. Investigation of Electrochemical Calcium-Ion Energy Storage Mechanism in Potassium Birnessite. *J. Power Sources* **2018**, *390*, 127−133.
(230) Suzuki, S.; Kato, T.; Kawabata, H.; Miyayama, M. Electrode Properties of Todorokite-Type Tunnel-Structured Manganese Oxide for Calcium Secondary Batteries. *J. New Mater. Electrochem. Syst.* **2016**, *19*, 51−55.
(231) Padigi, P.; Kuperman, N.; Thiebes, J.; Goncher, G.; Evans, D.; Solanki, R. Calcium Cobalt Hexacyanoferrate Cathodes for Rechargeable Divalent Ion Batteries. *J. New Mater. Electrochem. Syst.* **2016**, *19*, 57−64.
(232) Rogosic, J. Towards the Development of Calcium Ion Batteries. Ph.D. Thesis, Department of Materials Science and Engineering, Massachusetts Institute of Technology, 2014.

DOI: 10.1021/acs.chemrev.9b00339
Chem. Rev. 2020, 120, 6331−6357